

Polyoxometalate-Induced ‘Cage-within-Cage’ Metal Organic Frameworks with High Efficiency of CO₂ Photoreduction

*Ze-Yu Du,^a Yan-Zhao Yu,^a Ning-Fang Li,^a Yun-Shan Xue,^a Ling-Xi Xu,^b Hua Mei^{*a} and Yan Xu^{*a}*

Corresponding authors: Yan Xu and Hua Mei

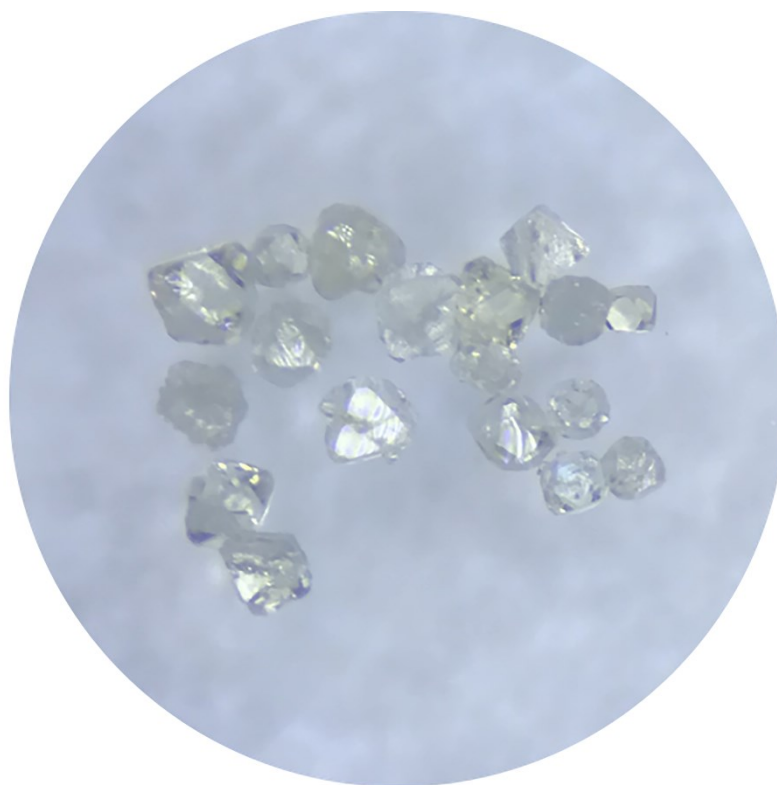
E-mails: yanxu@njtech.edu.cn and meihua@njtech.edu.cn

Contents

Section 1. Crystal Structure.....	3
Section 2. Characterizations	18
XRD.....	19
IR.....	21
TG	22
SEM	23
EDS-Mapping	24
ICP	24
BET	25
CO₂ Adsorption	27
Section 3. The Procedure of the CO₂ Photoreduction.....	28
Reaction	32
GC profile.....	33
XRD.....	35
Section 4. Other Tables.....	36
Reference.....	40

Section 1. Crystal Structure

(a)



(b)

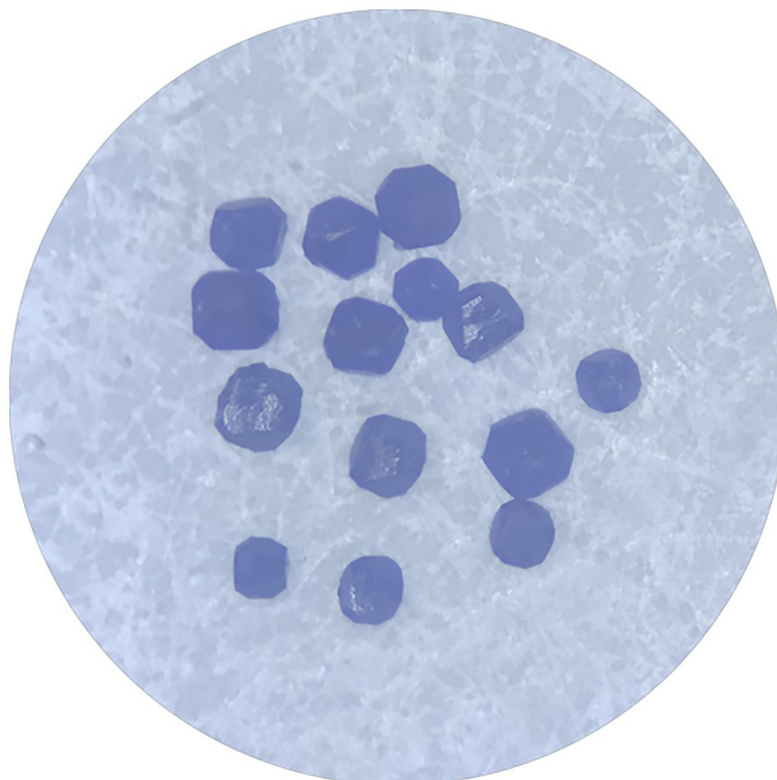


Figure S1. (a) The crystal image of **Zn/Mo-MOF** under optical microscope; (b) the crystal image of **Zn/Co/Mo-MOF** under optical microscope.

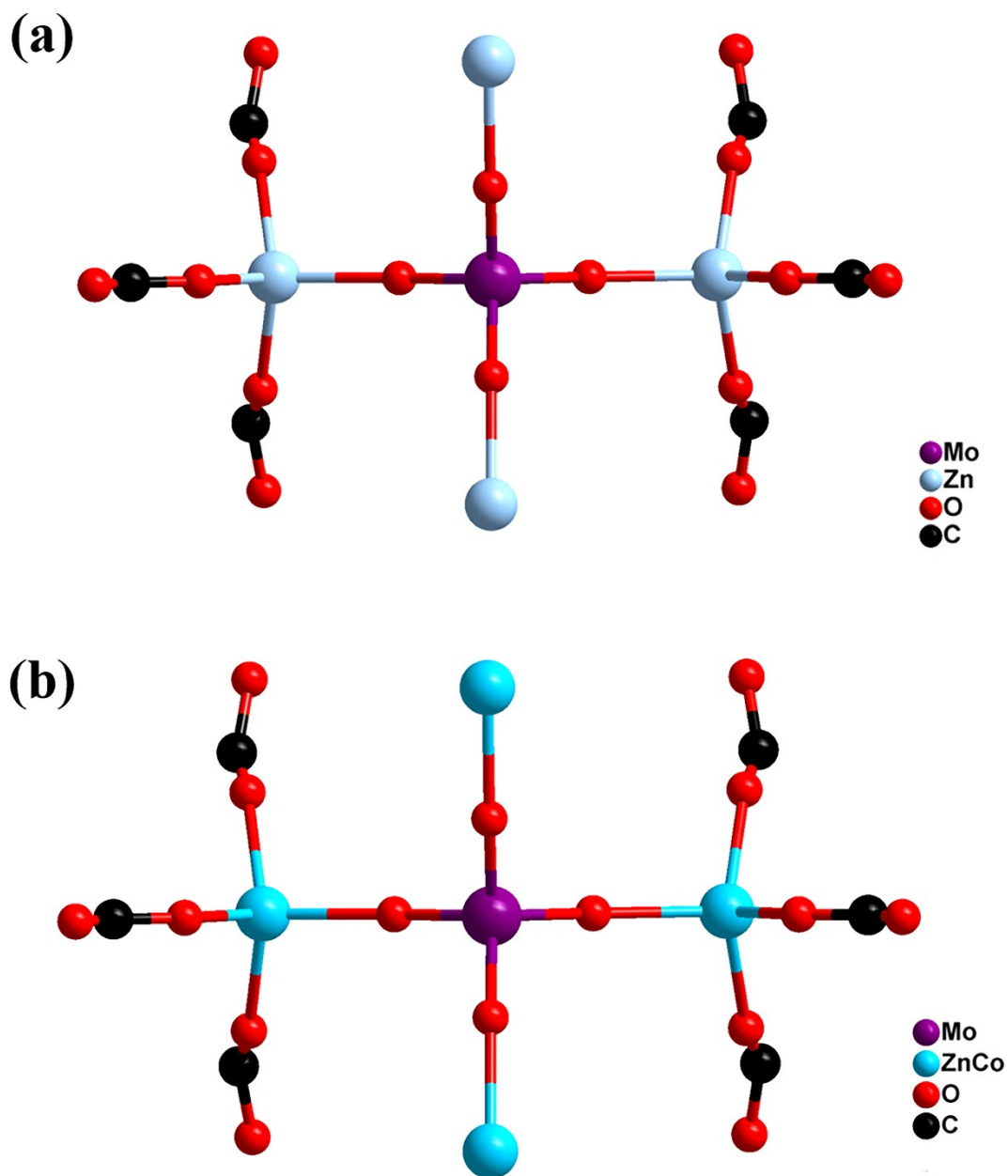
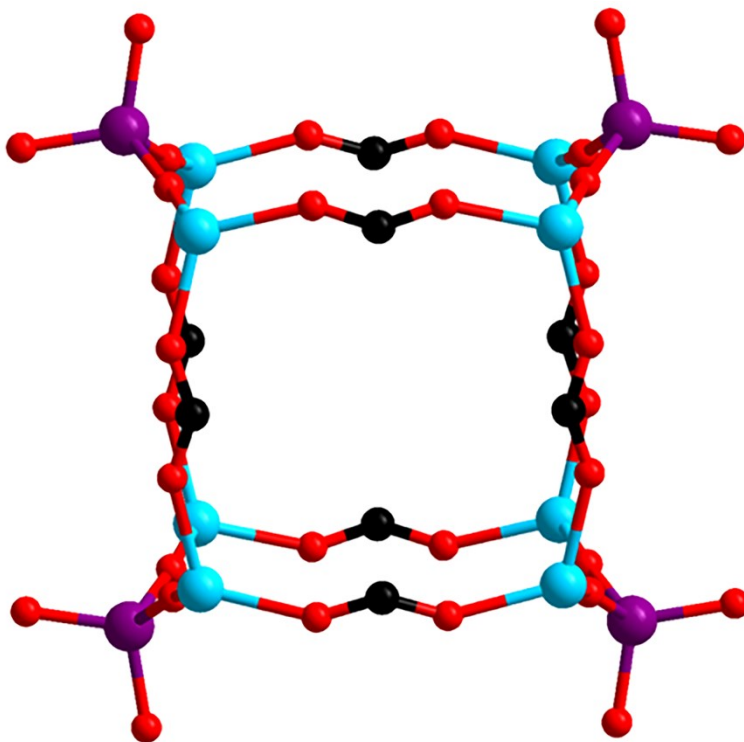


Figure S2. (a) Stick representation of basic unit for **Zn/Mo-MOF**; (b) stick representation of basic unit for **Zn/Co/Mo-MOF**. All organic ligands are expressed as HCOO^- and hydrogen atoms are omitted for clarity.

(a)



(b)

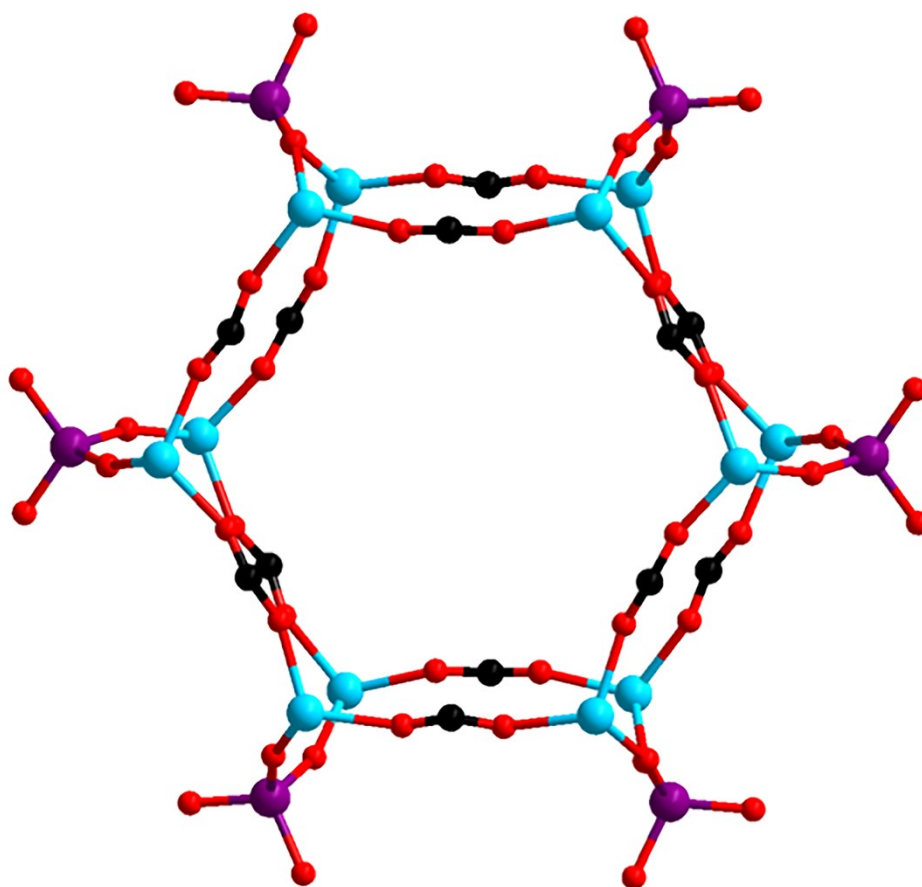


Figure S3. (a) Ball-and-stick representations showing the linkage of 4-ring; (b) ball-and-stick representations showing the linkage of 6-ring. All organic ligands are expressed as HCOO^- and hydrogen atoms are omitted for clarity.

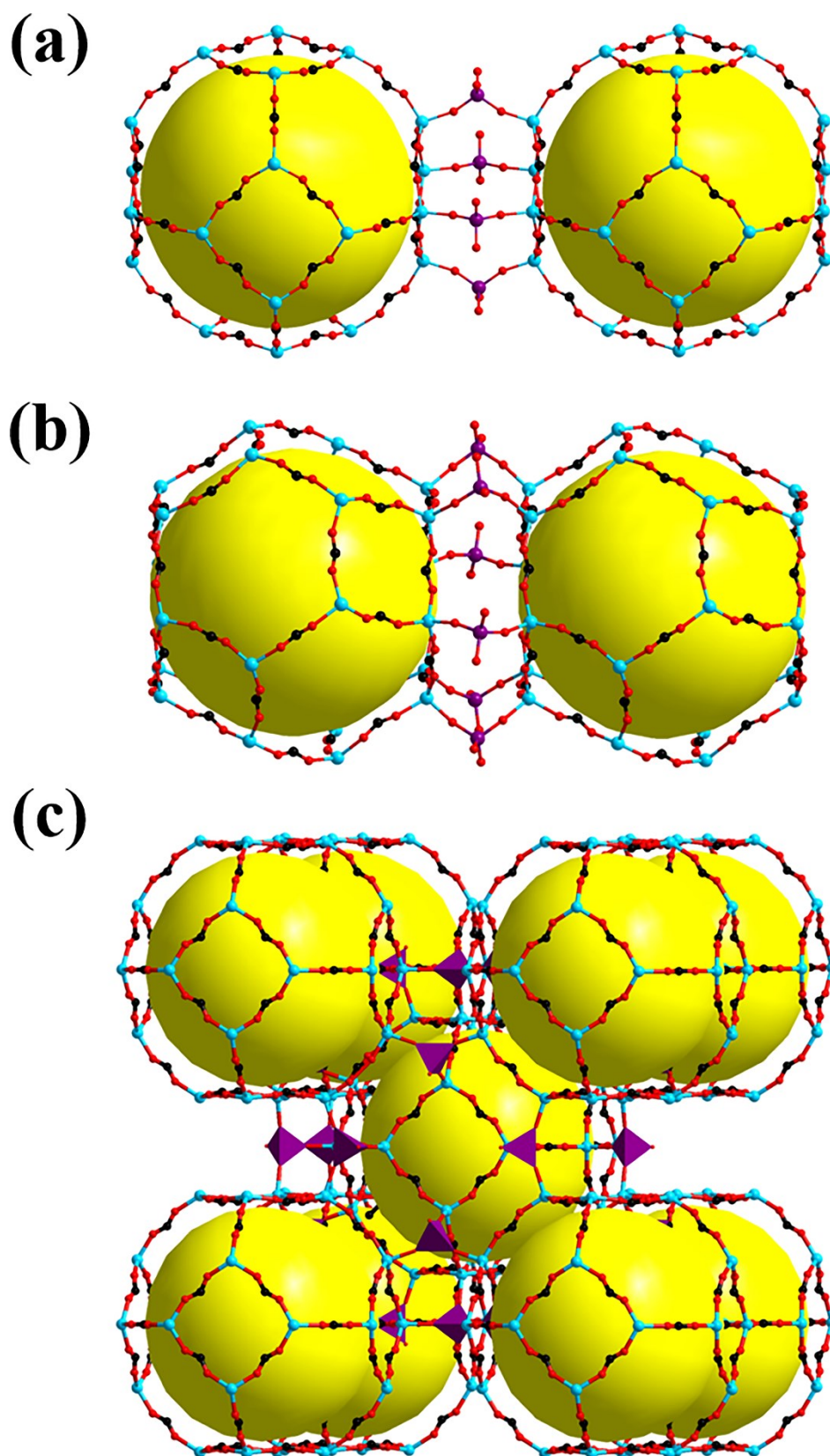


Figure S4. (a)/(b)/(c) Ball-and-stick representations showing the linkage of cage α . All organic ligands are expressed as HCOO^- and hydrogen atoms are omitted for clarity.

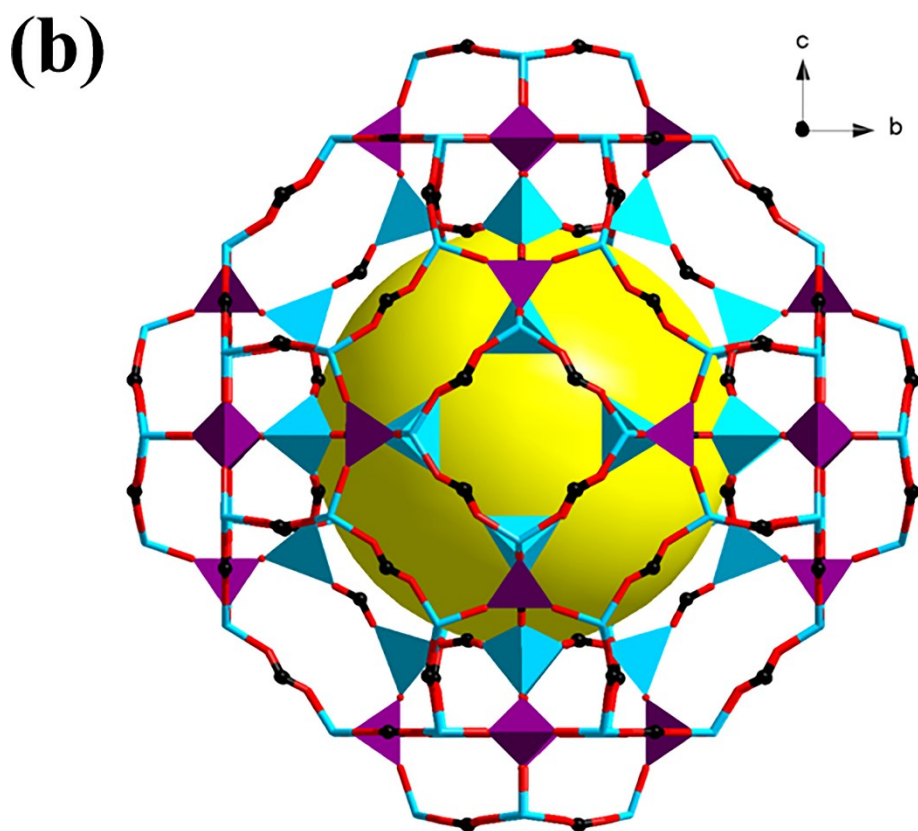
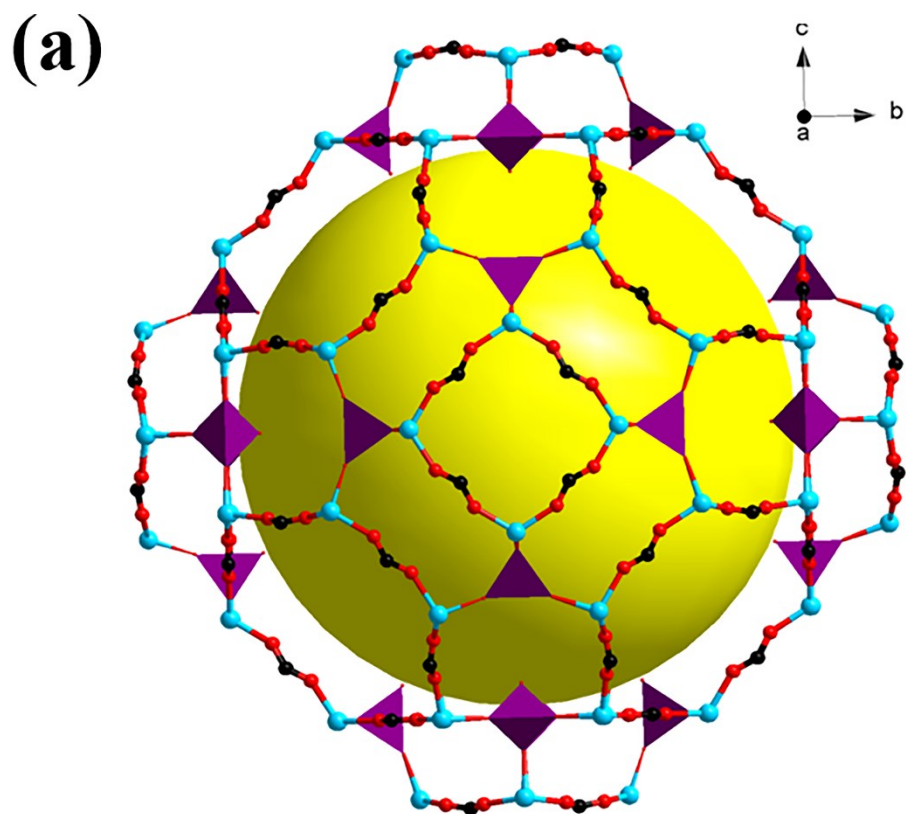


Figure S5. (a) Ball-stick and polyhedral representations of cage β along with a -axis; (b) ball-stick and polyhedral representations of cage $\alpha@ \beta$ along with a -

axis. All organic ligands are expressed as HCOO^- and hydrogen atoms are omitted for clarity.

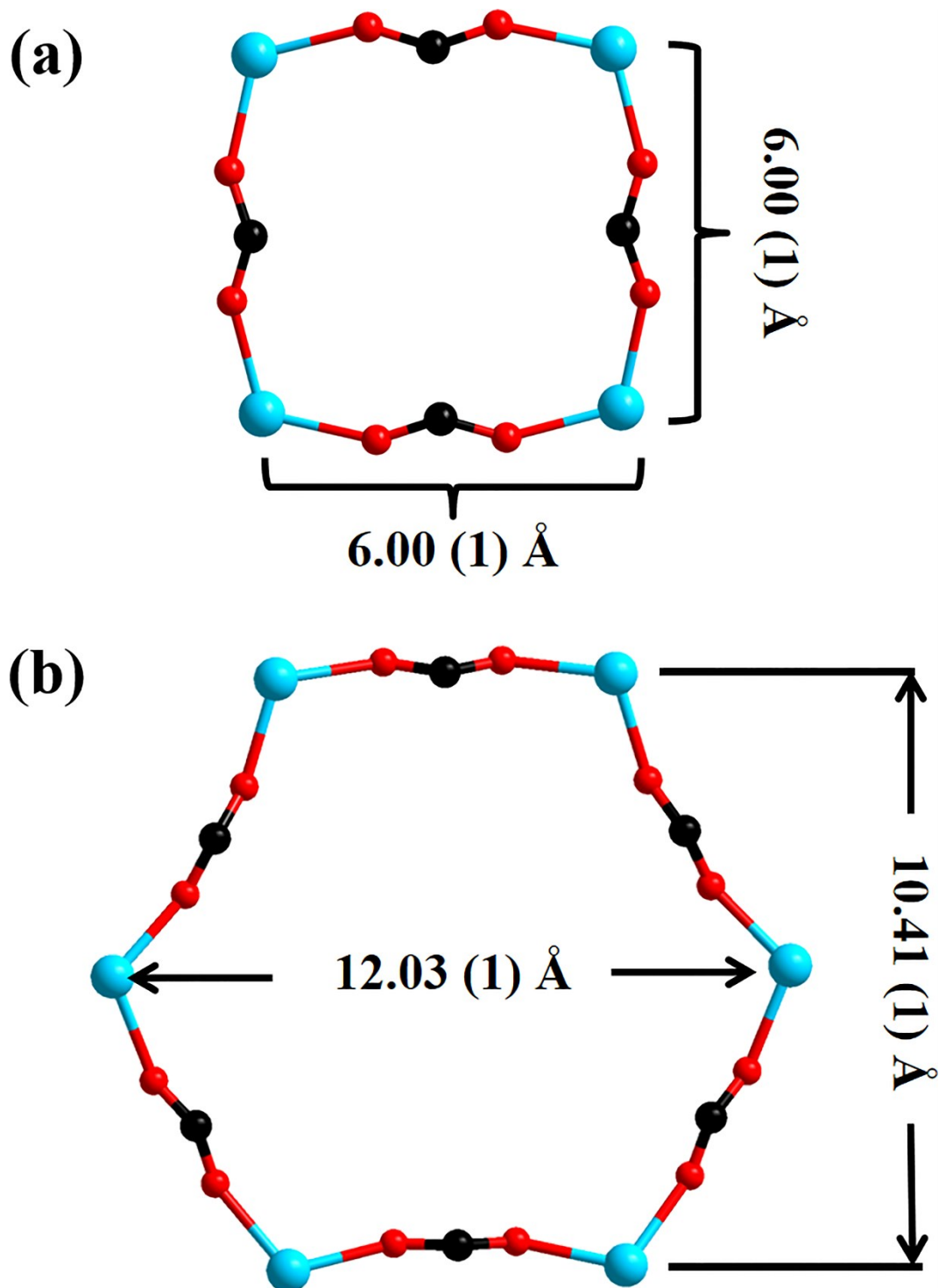


Figure S6. (a) Ball-and-stick representations of 4-ring; (b) ball-and-stick representations 6-ring. All organic ligands are expressed as HCOO^- and hydrogen atoms are omitted for clarity.

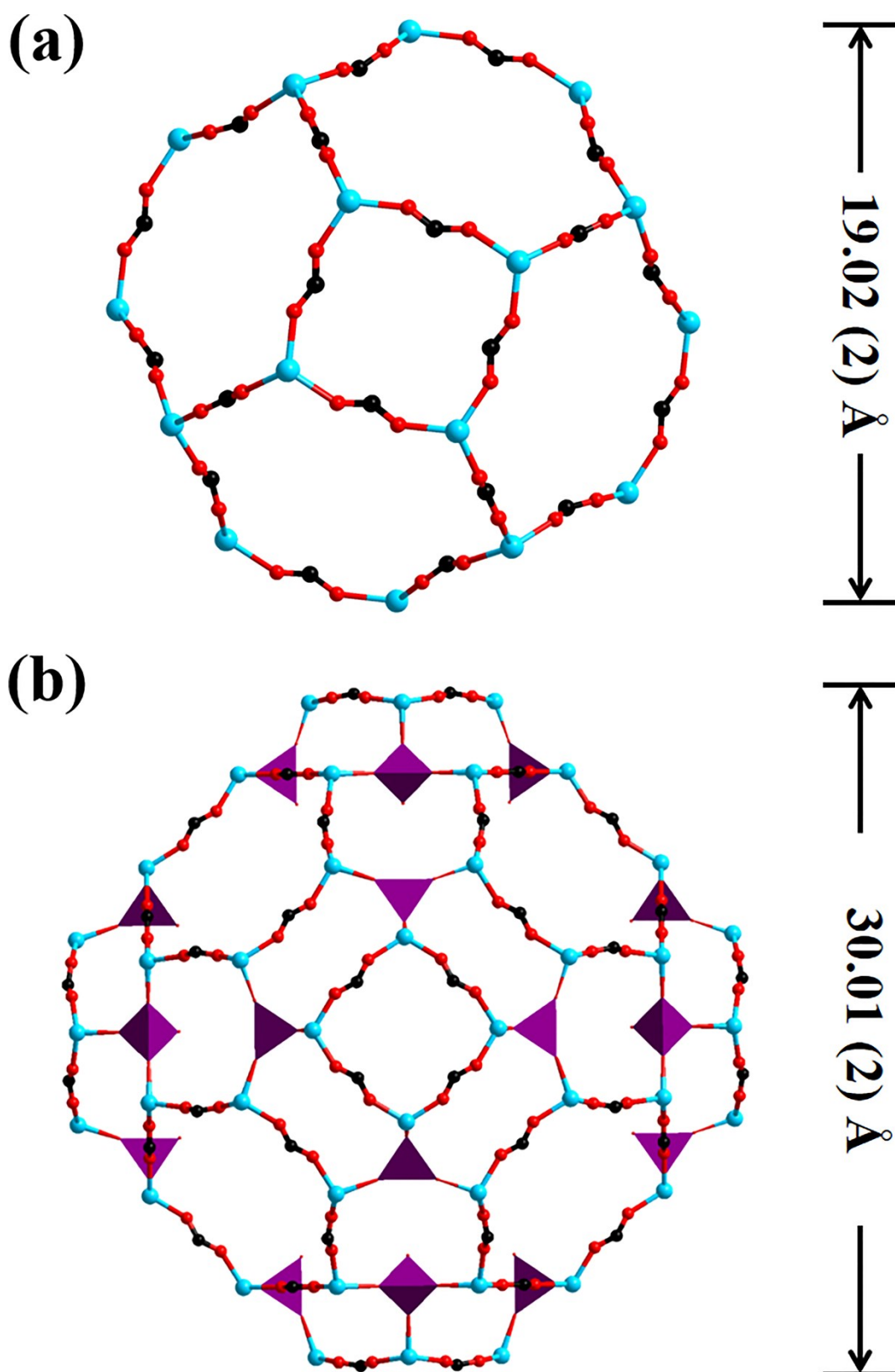


Figure S7. (a) Ball-and-stick representations of cage α ; (b) ball-stick representations of cage β . All organic ligands are expressed as HCOO^- and hydrogen atoms are omitted for clarity.

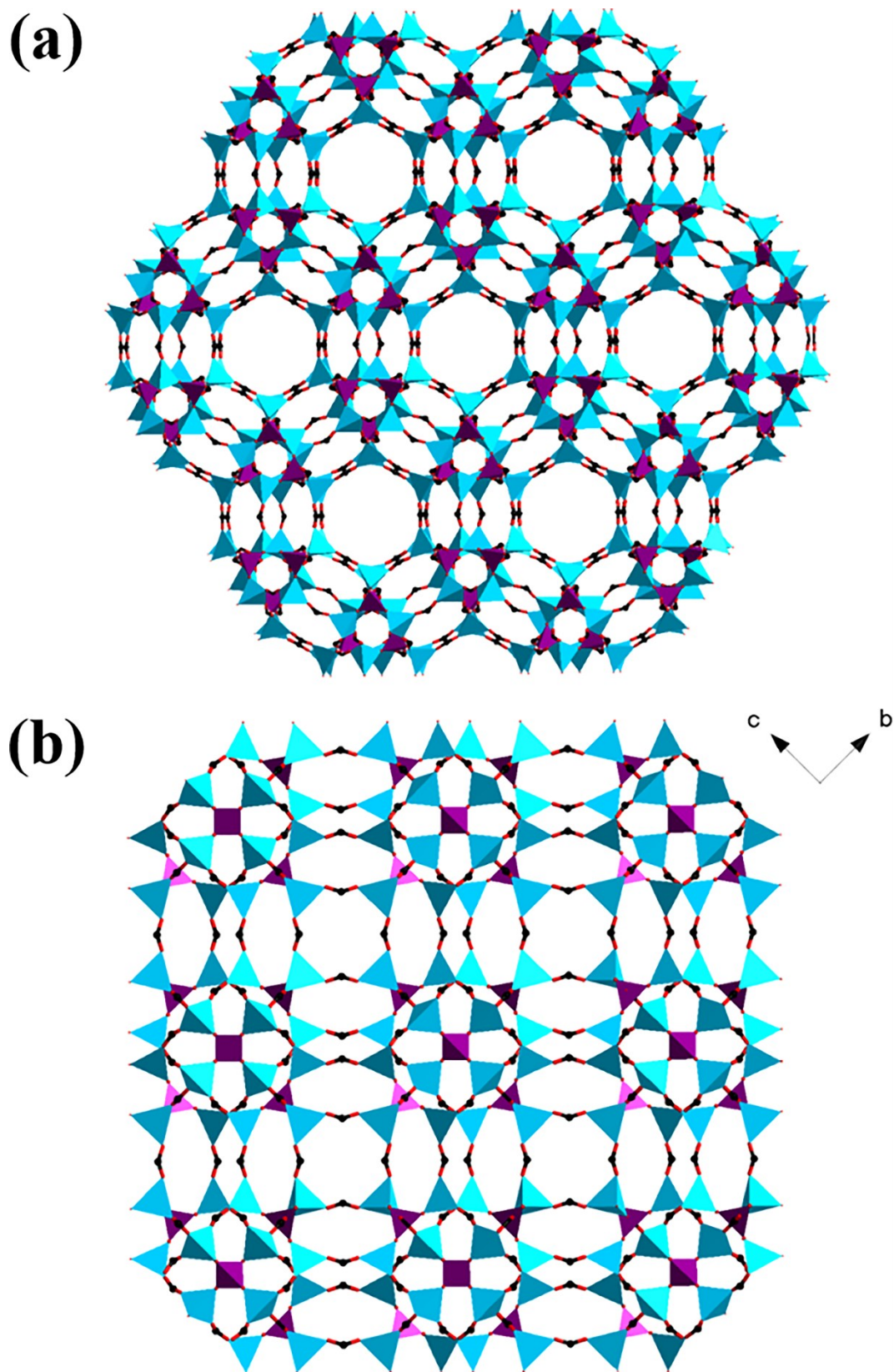


Figure S8. (a) Ball-stick and polyhedral views of 3D structure in **Zn/Co/Mo-MOF**; (b) stick and polyhedral views of 3D structure in **Zn/Co/Mo-MOF** along with *a*-axis. All organic ligands are expressed as HCOO^- and hydrogen atoms

are omitted for clarity

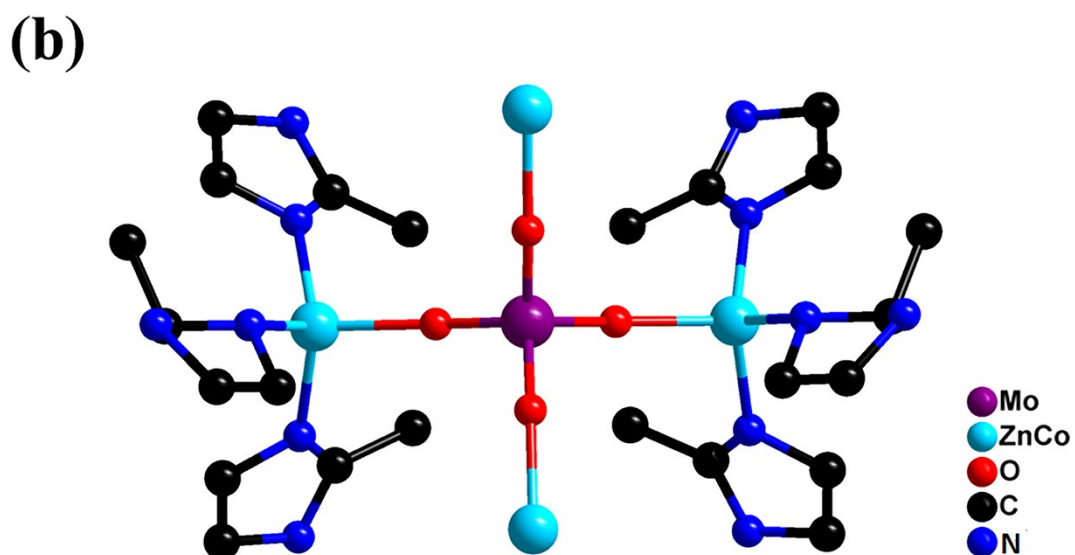
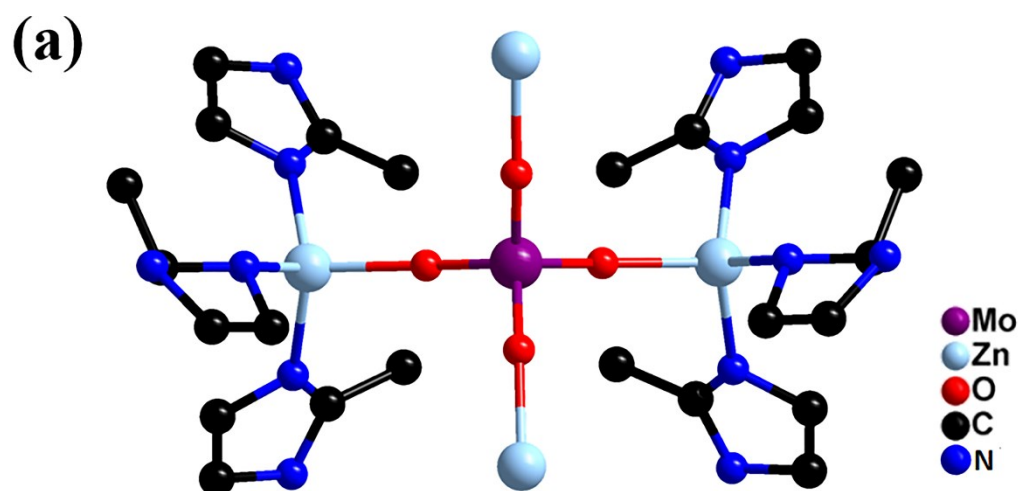


Figure S9. (a) Ball-and-stick representation of basic unit for **Zn/Mo-MOF**; (b) ball-and-stick representation of basic unit for **Zn/Co/Mo-MOF**. All organic ligands are expressed as 2-methylimidazole and hydrogen atoms are omitted for clarity.

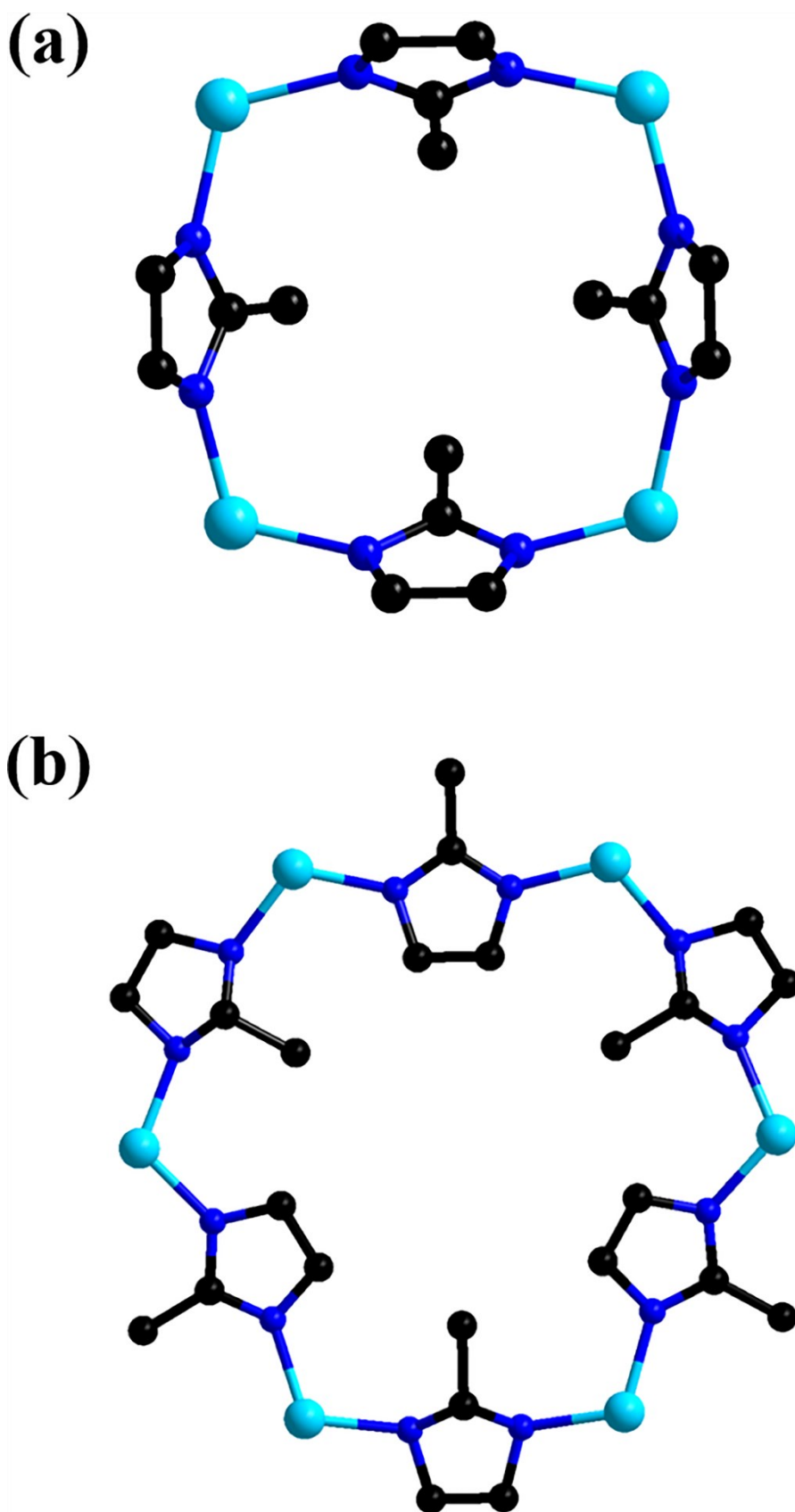
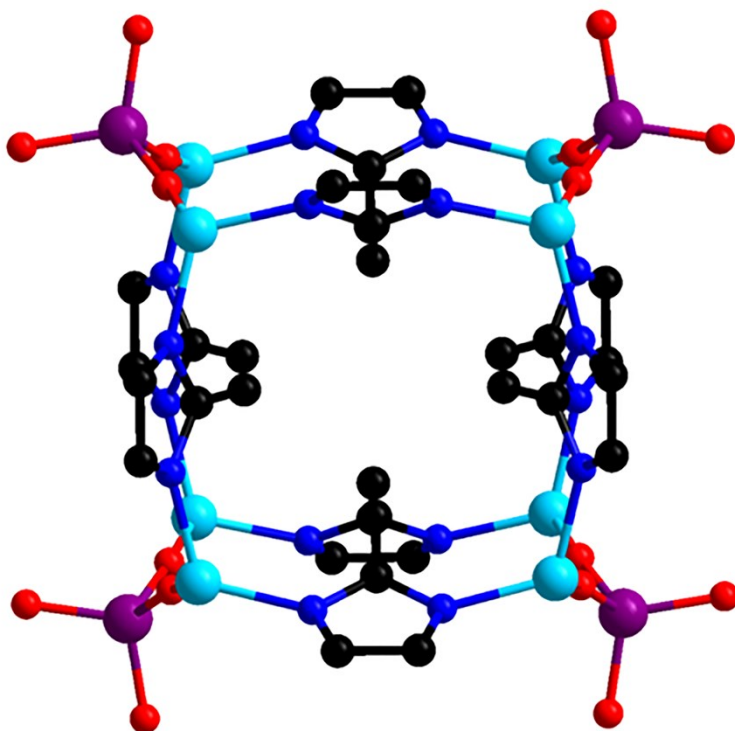


Figure S10. (a) Ball-and-stick representations of 4-ring; (b) ball-and-stick representations 6-ring. All organic ligands are expressed as 2-methylimidazole and hydrogen atoms are omitted for clarity.

(a)



(b)

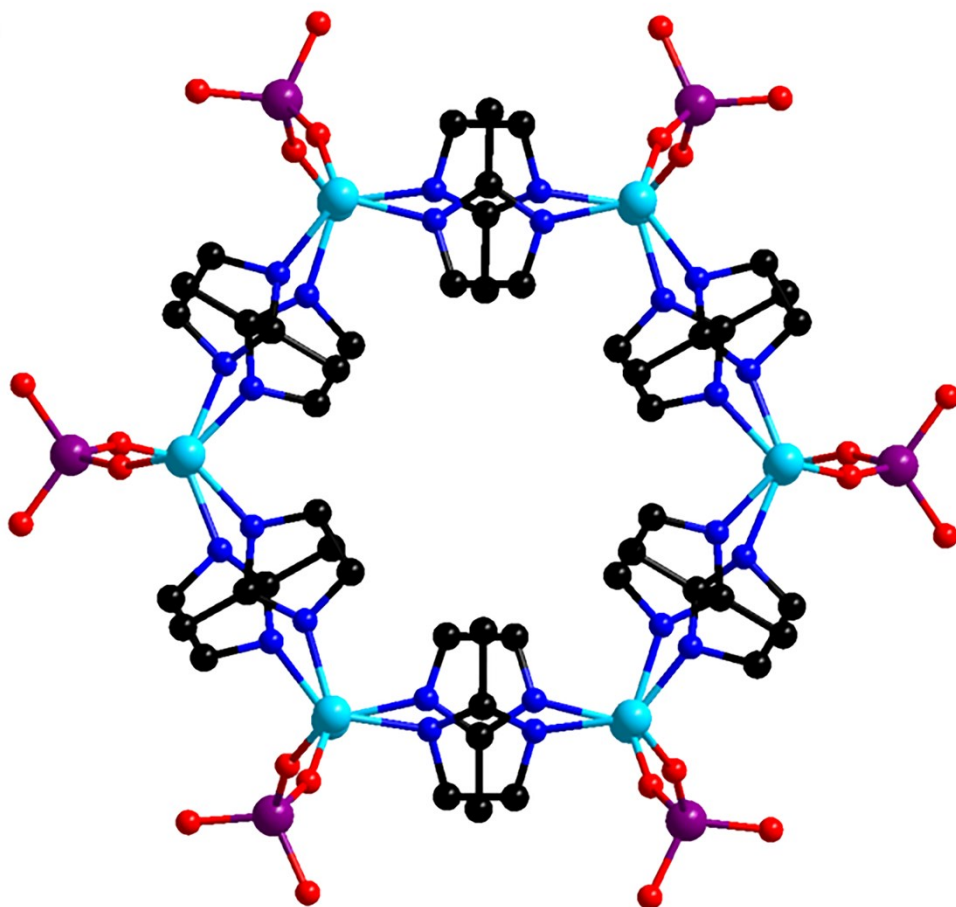
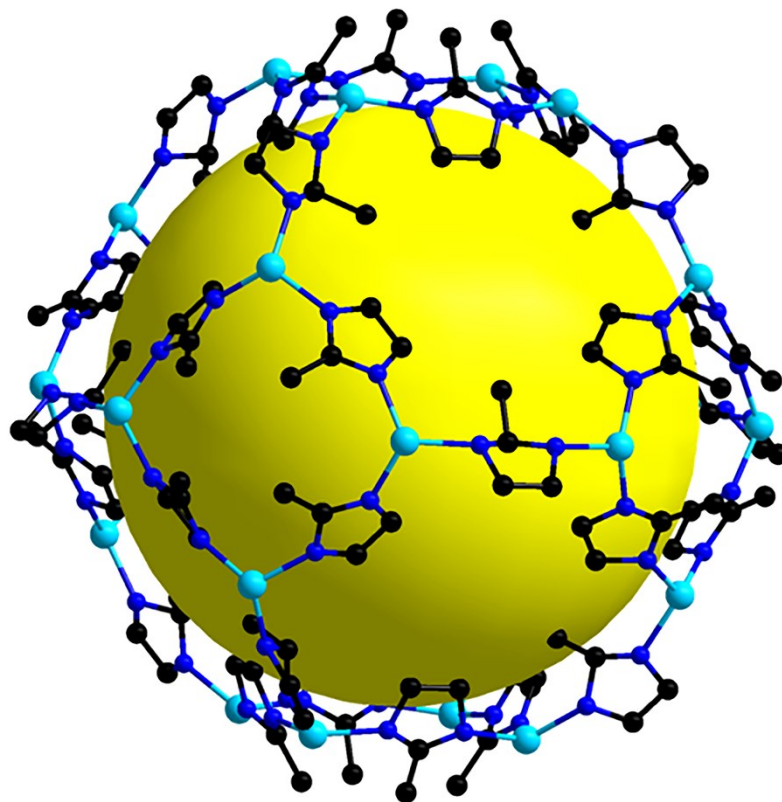


Figure S11. (a) Ball-and-stick representations showing the linkage of 4-ring; (b) ball-and-stick representations showing the linkage of 6-ring. All organic ligands are expressed as 2-methylimidazole and hydrogen atoms are omitted for clarity.

(a)



(b)

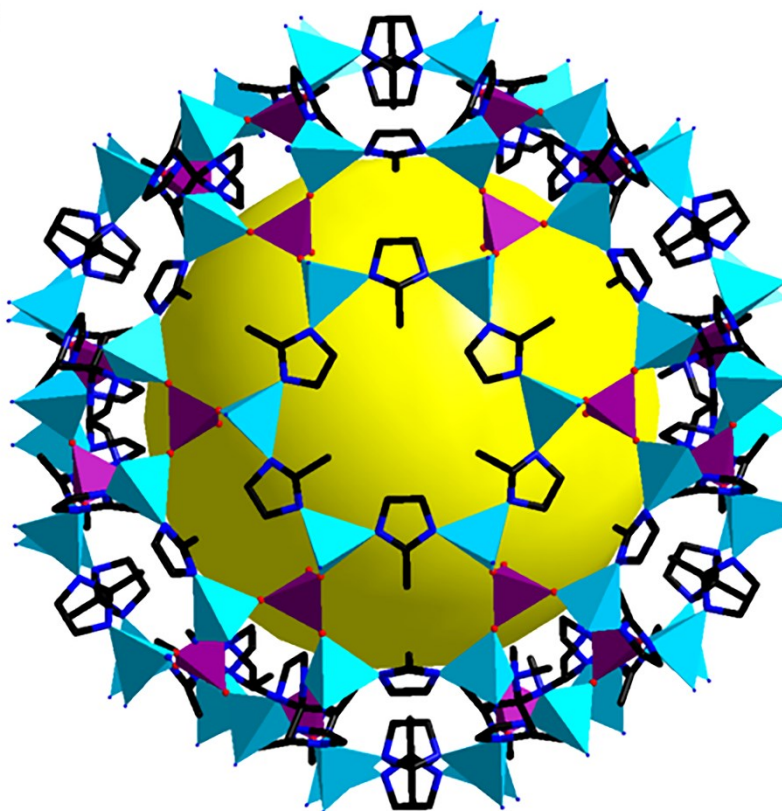
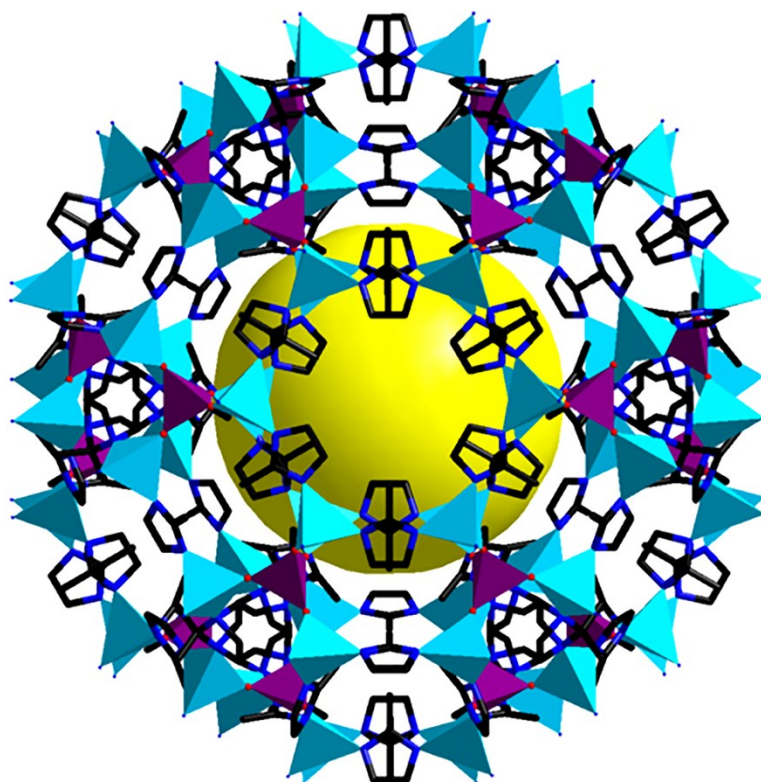


Figure S12. (a) Ball-and-stick representations of cage α ; (b) Stick and polyhedral representations of cage β . All organic ligands are expressed as 2-methylimidazole and hydrogen atoms are omitted for clarity.

(a)



(b)

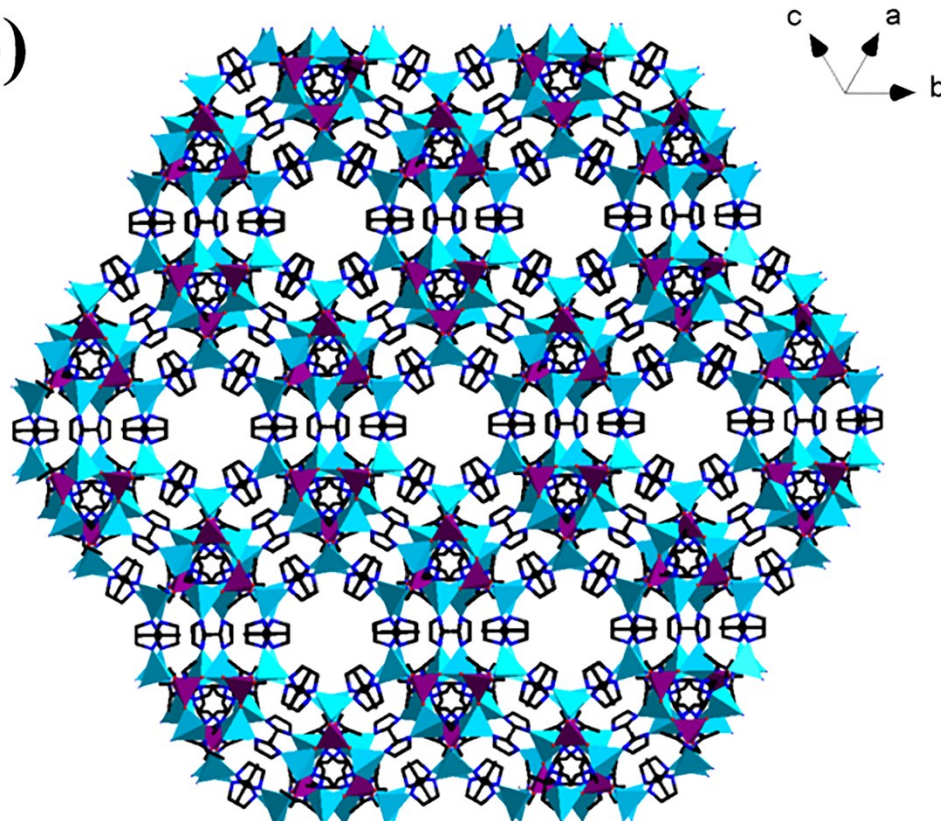
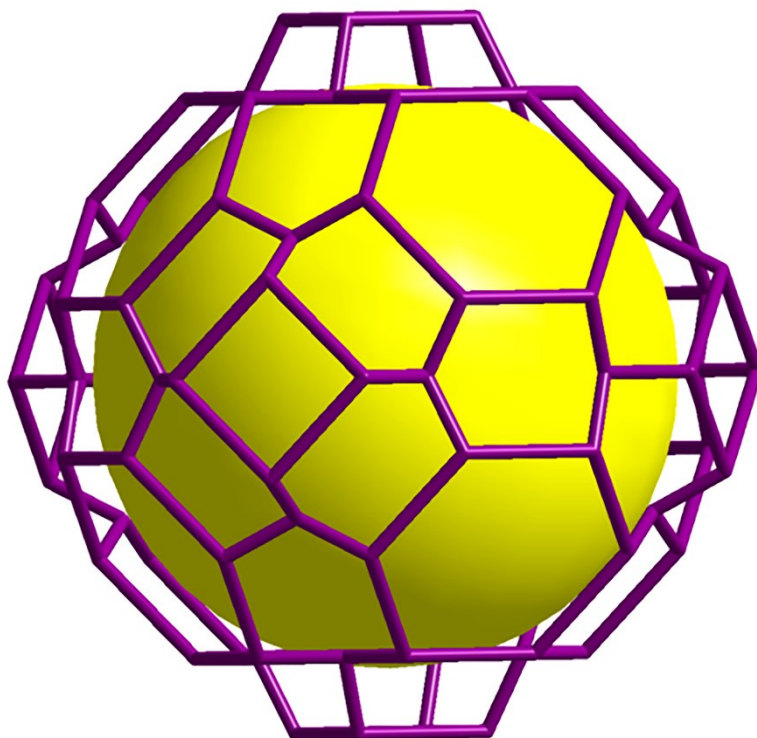


Figure S13. (a) Stick and polyhedral views of $\alpha@beta$; (b) stick and polyhedral views of three-dimensional structure in Zn/Co/Mo-MOF. All organic ligands are expressed as 2-methylimidazole and hydrogen atoms are omitted for clarity.

(a)



(b)

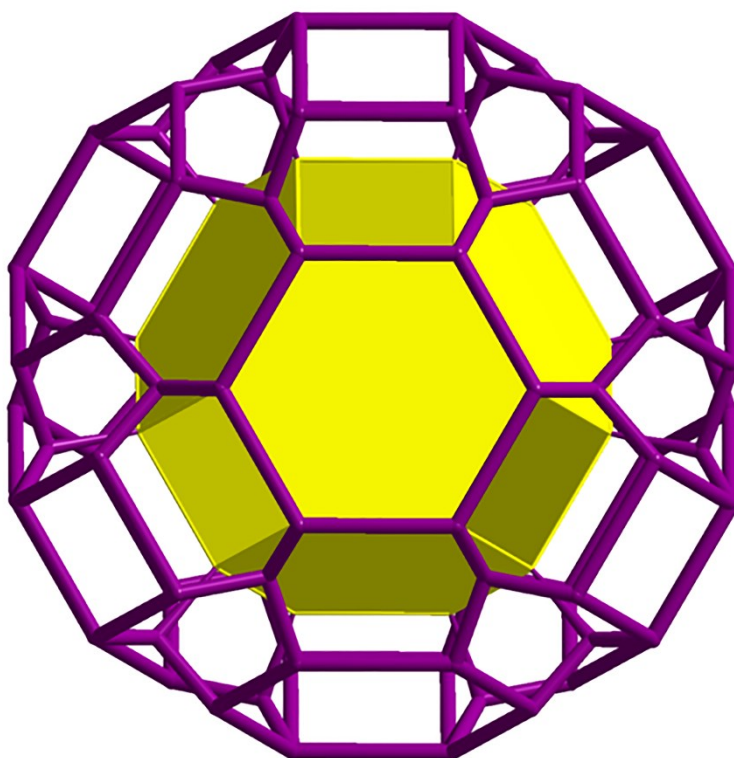
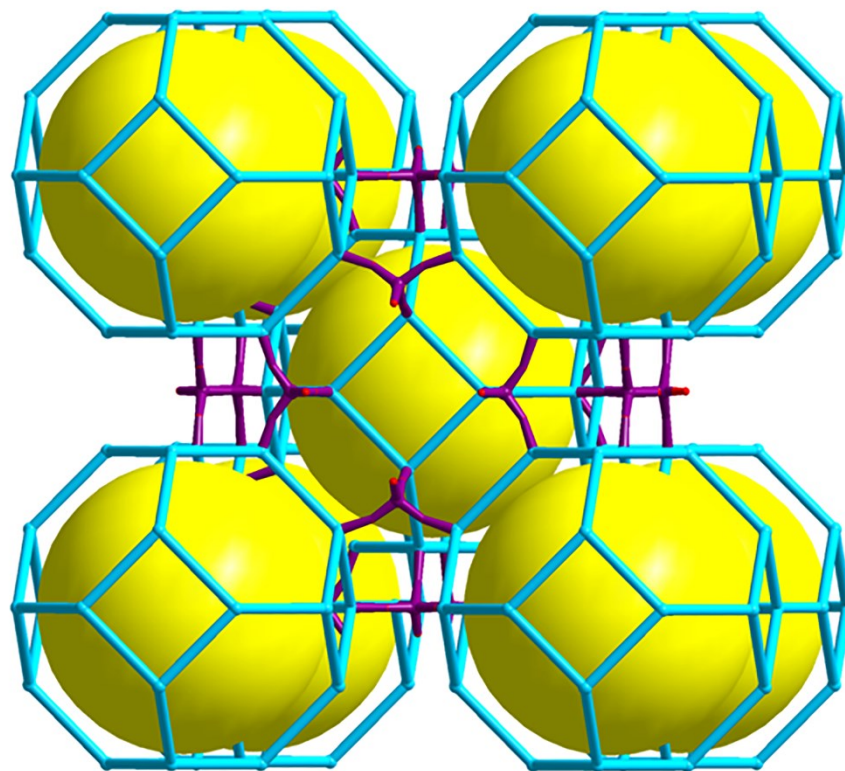


Figure S14. (a) Topological features of **cage β** ; (b) topological features of **cage $\alpha@ \beta$** .

(a)



(b)

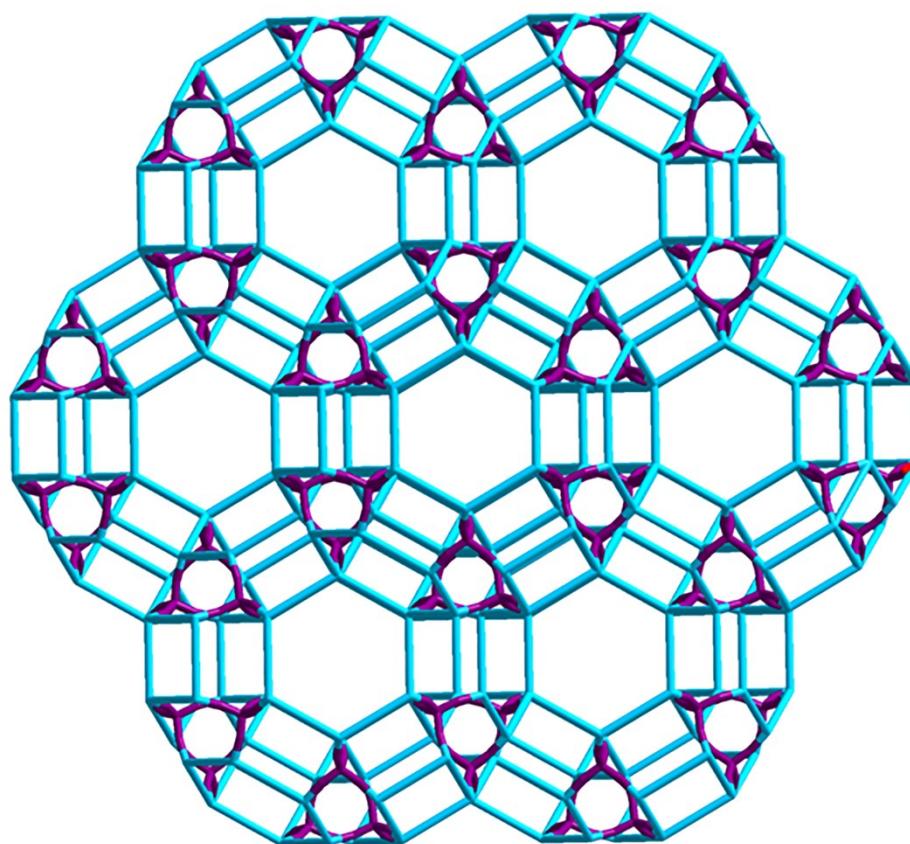


Figure S15. (a) Sodalite topology of two MOFs; (b) 3D topology of two MOFs.

Section 2. Characterizations

Materials and Physical property studies.

X-ray diffraction (PXRD) data of two MOFs was completed on Smartlab TM 9KW diffractometer using Cu K α radiation ($\lambda = 1.54056$ nm), and the range was 3 to 50 °. FTIR spectrums were carried out on Nicolet 470 FTIR spectrometer with KBr pellets in the 400 - 4000 cm⁻¹ range. Powder Thermogravimetric analysis (TGA) was carried out on STA449F3 thermogravimetric analyzer in N₂ atmosphere with a heating rate of 10 °C/min. The UV-vis diffuse reflectance spectra were completed on SHIMADZU UV-2600 spectrophotometer, and the wavelength was in range of 200–800 nm. The SEM and EDS-mapping were identified by using a Hitachi TM 3000 scanning electron microscope at an accelerating voltage of 20 kV. Elemental analyses (C, N and H) were determined by a Perkin-Elmer 2400 elemental analyzer. The contents of relevant elements (Zn, Co, and Mo) of the two MOFs were measured by inductively coupled plasma atomic emission spectroscopy (ICP-AES) using an OPTMA20000V spectrometer. N₂ gas adsorption and desorption isotherms and CO₂ gas adsorption isotherms were performed on BELSORP-max gas adsorption instrument.

XRD

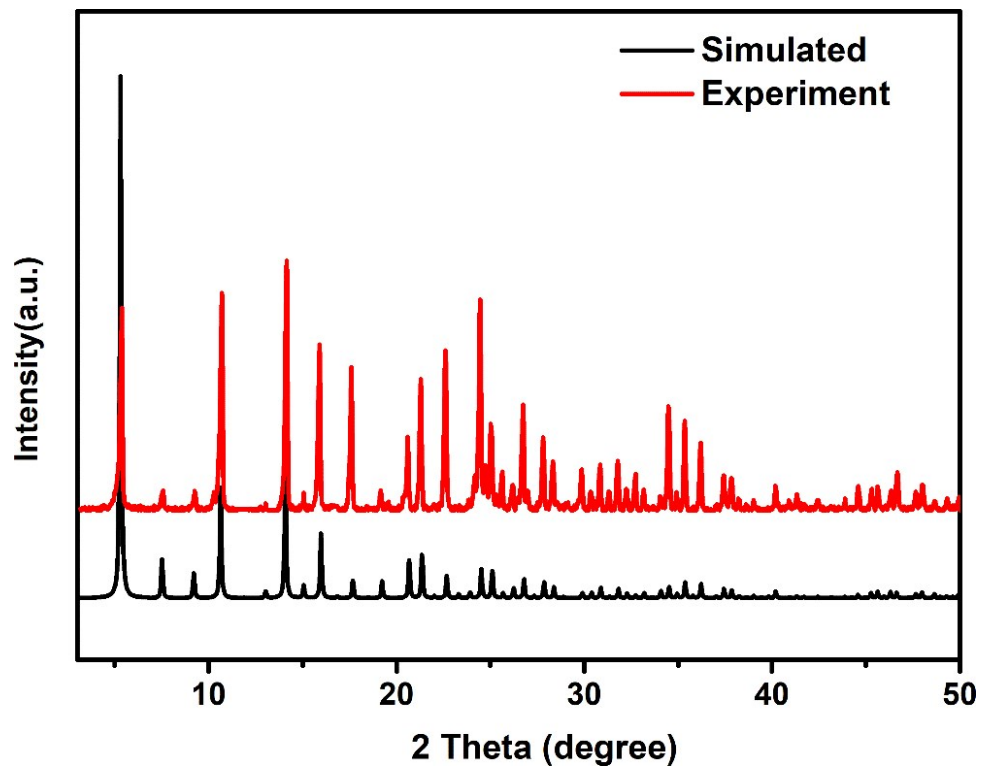


Figure S16. (a) The XRD pattern of Zn/Mo-MOF.

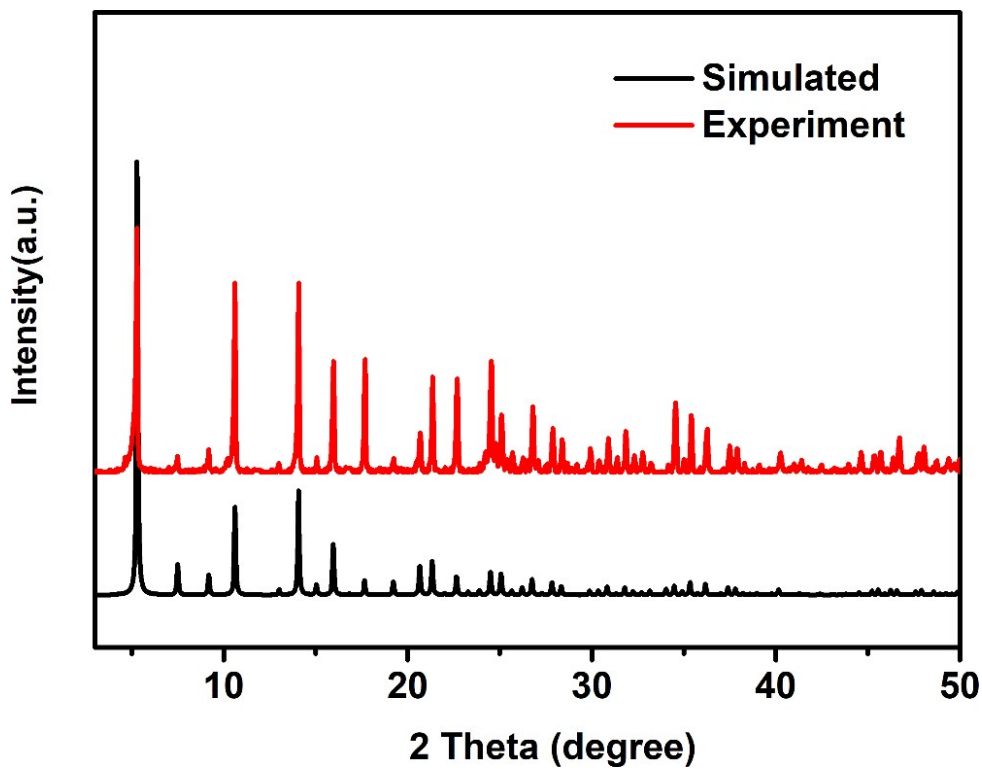


Figure S17. (a) The XRD pattern of Zn/Co/Mo-MOF.

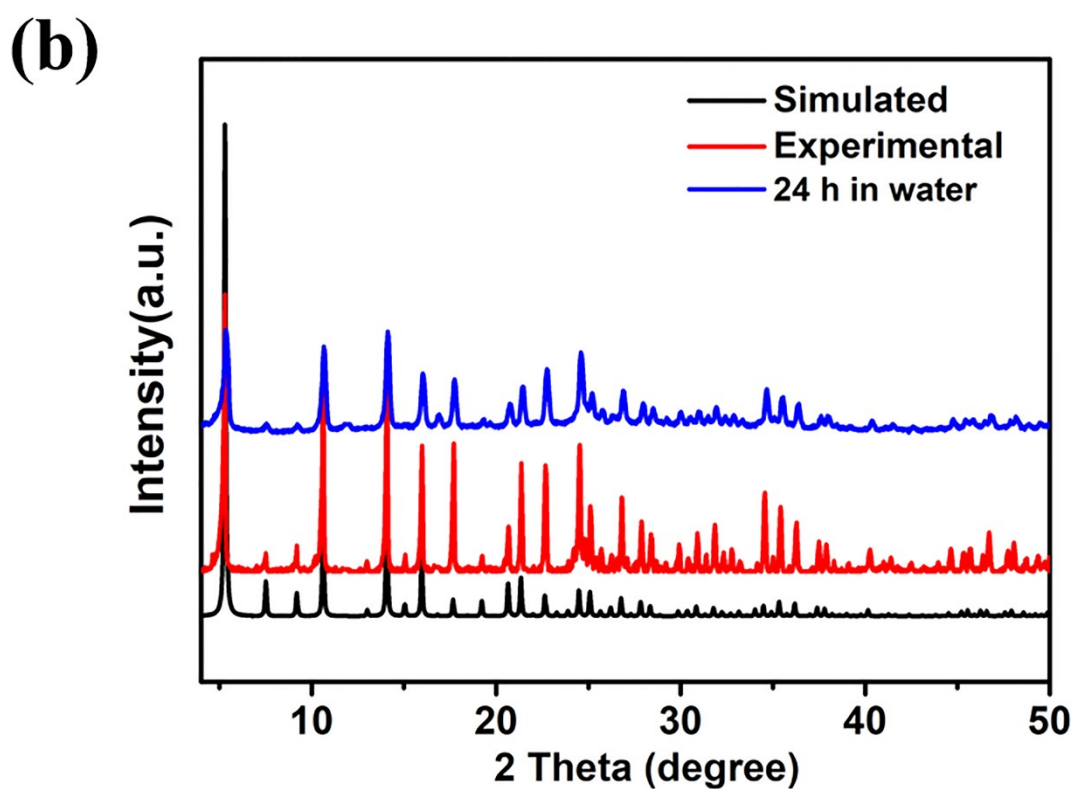
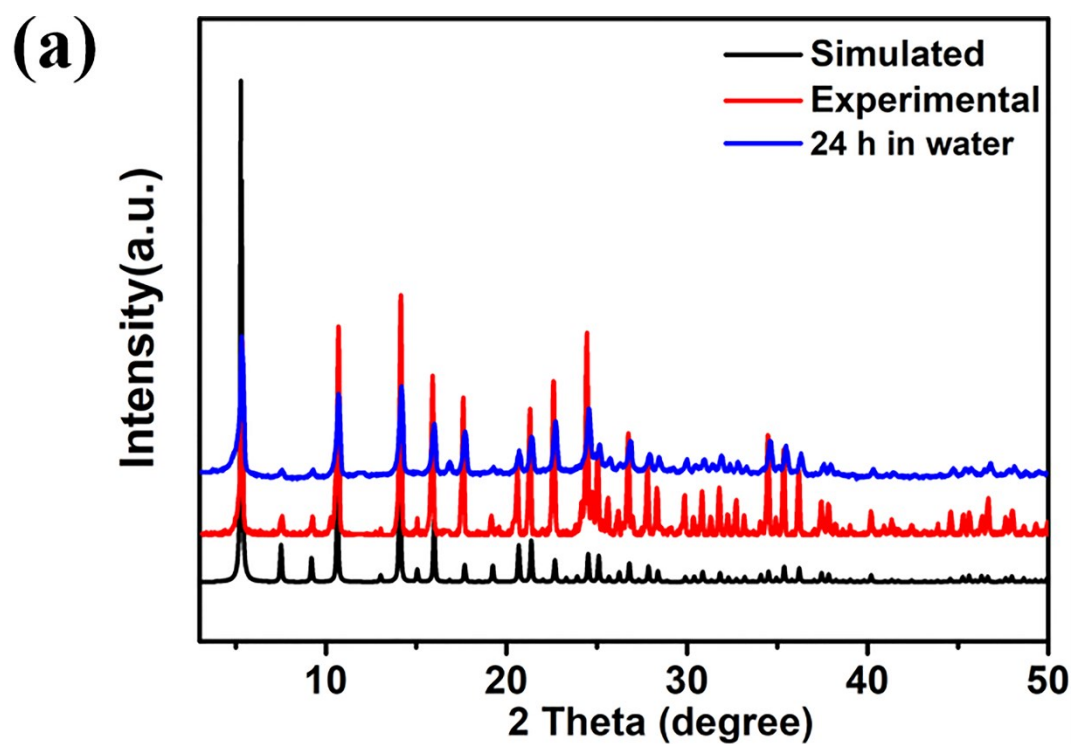


Figure S18. The XRD pattern of (a) Zn/Mo-MOF and (b) Zn/Co/Mo-MOF in water.

IR

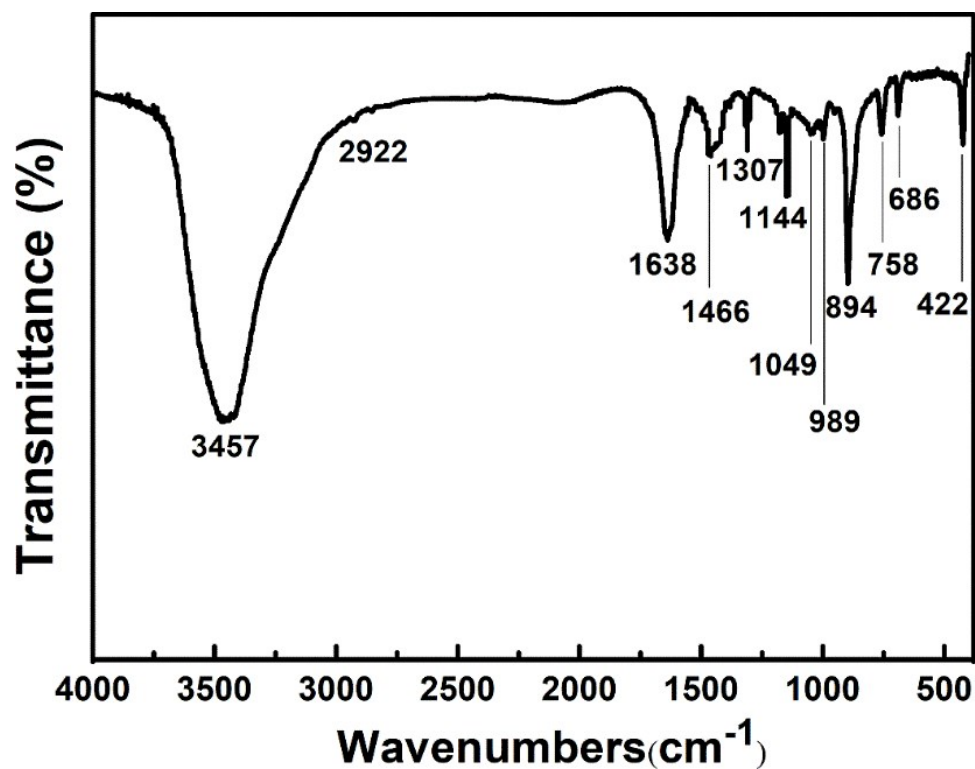


Figure S19. The IR spectra of Zn/Mo-MOF.

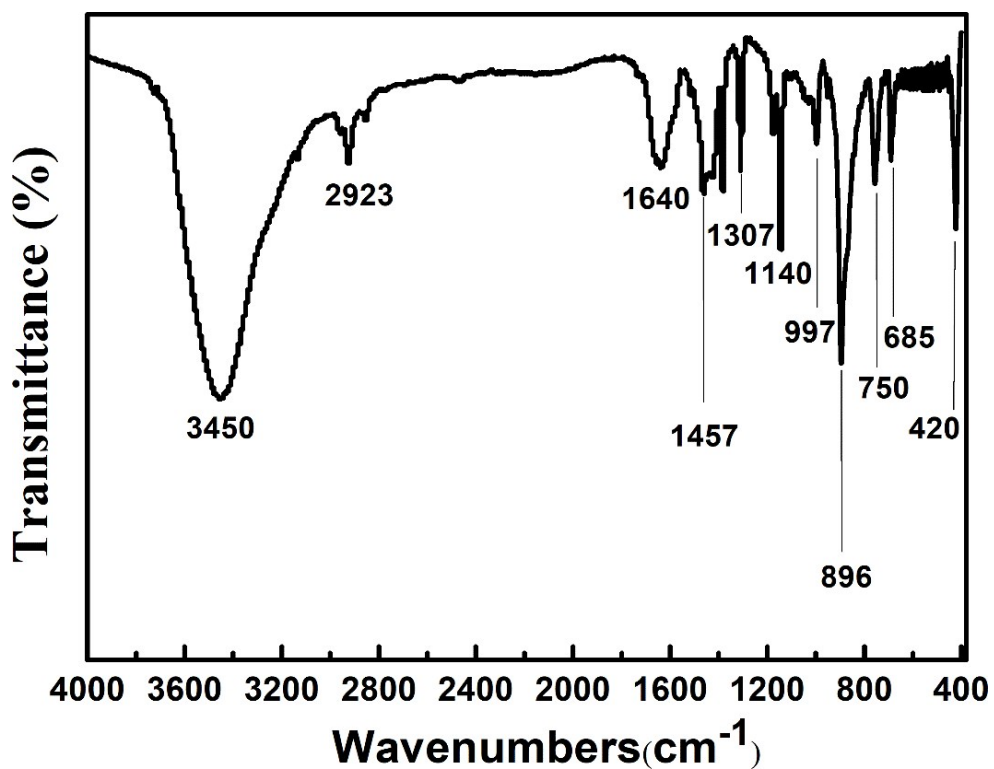


Figure S20. The IR spectra of Zn/Co/Mo-MOF.

TG

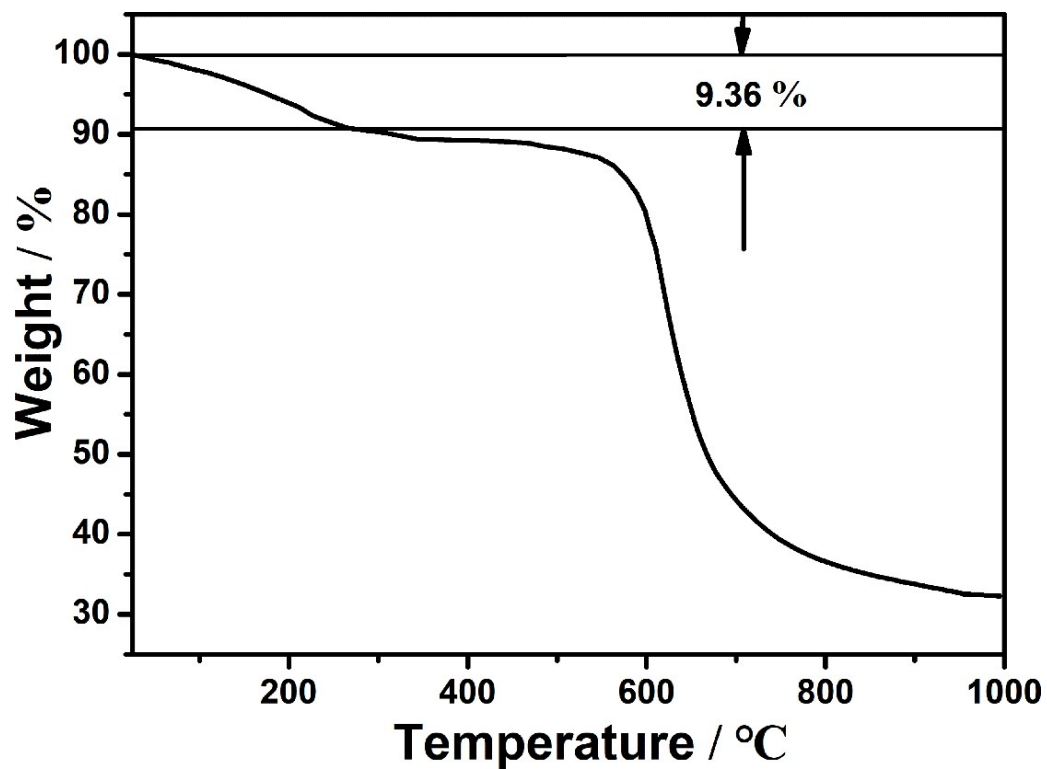


Figure S21. The TG spectra of Zn/Mo-MOF.

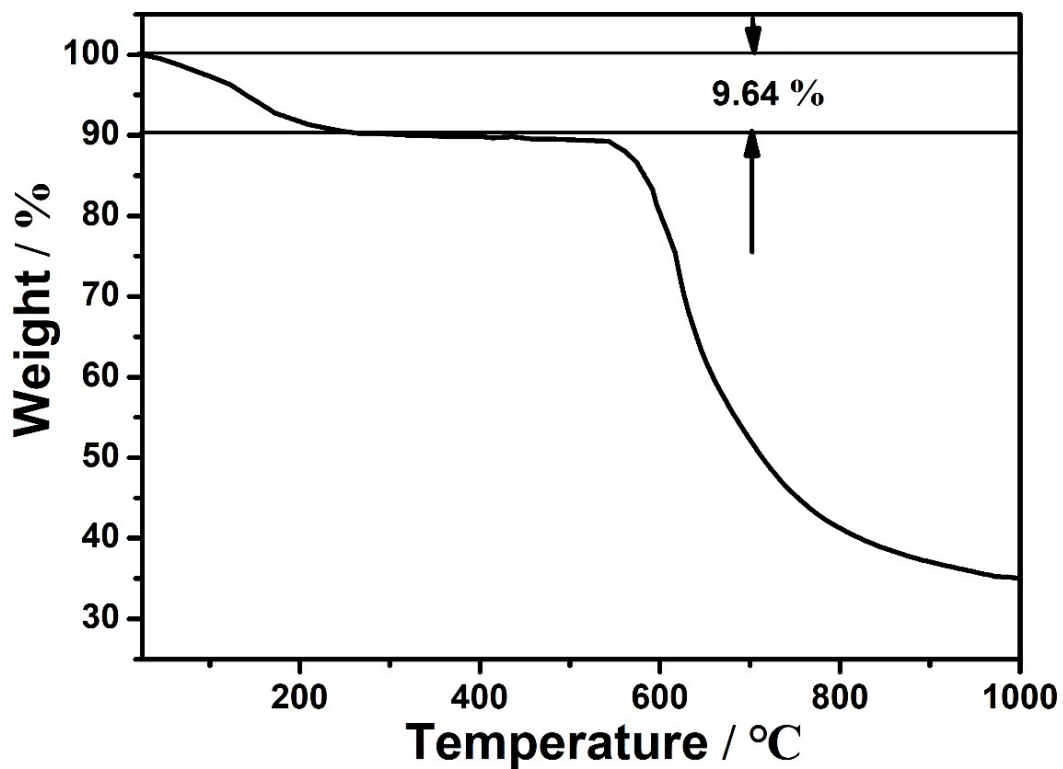


Figure S22. The TG spectra of Zn/Co/Mo-MOF.

SEM

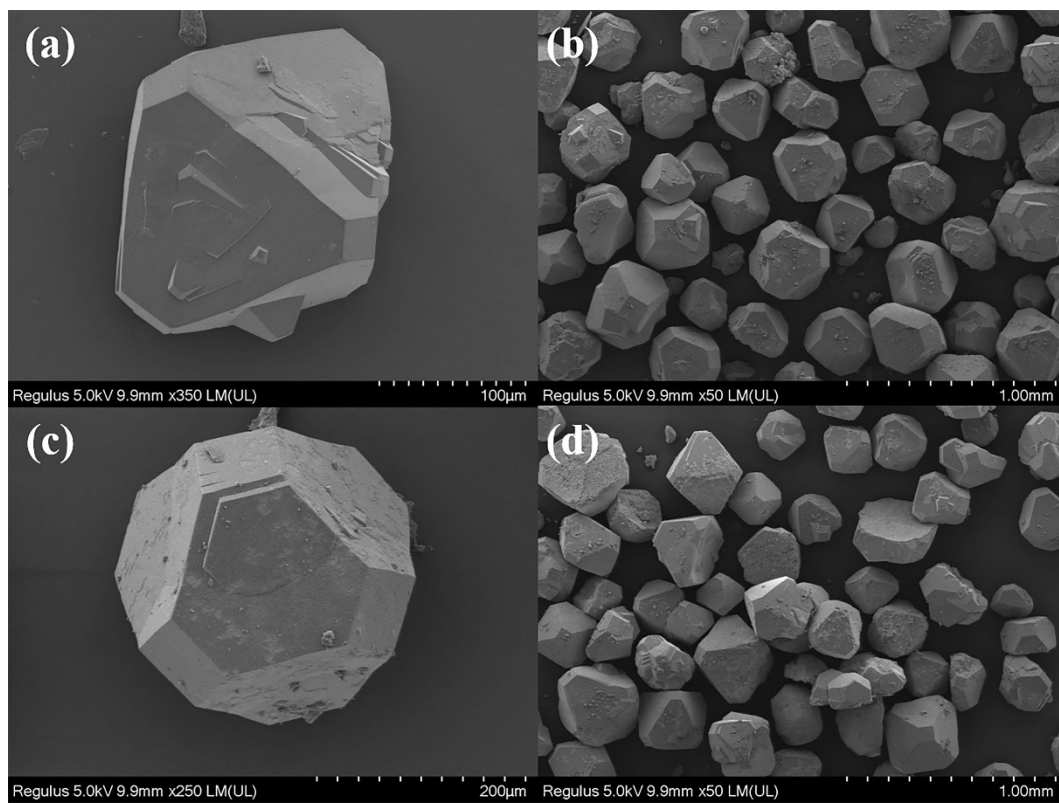


Figure S23. (a), (b) SEM images of **Zn/Mo-MOF**; (c), (d) SEM images of **Zn/Co/Mo-MOF**.

EDS-Mapping

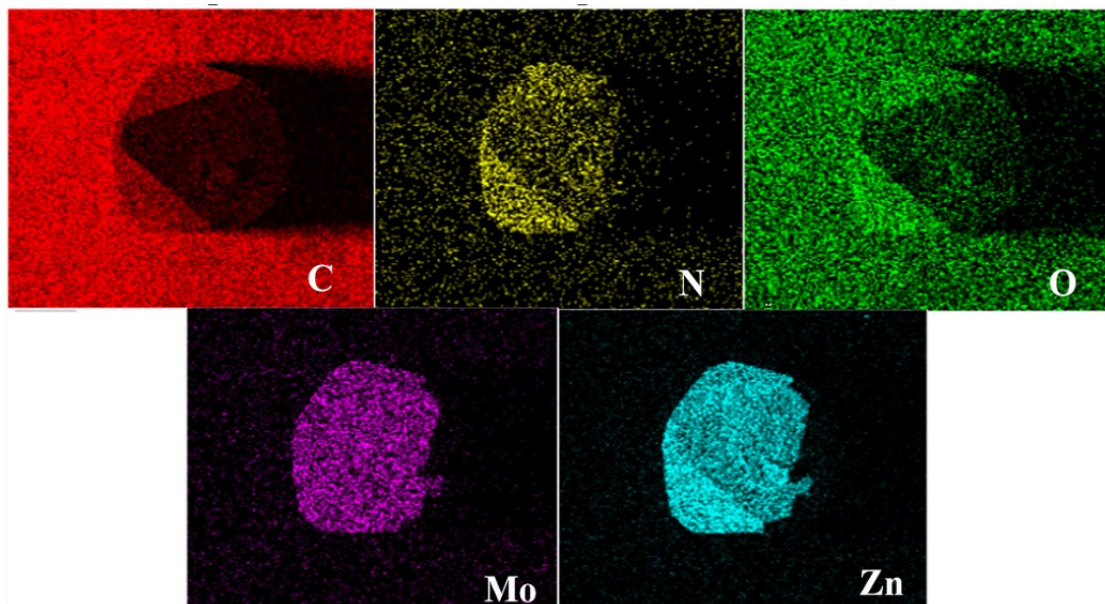


Figure S24. The EDS mapping of Zn/Mo-MOF.

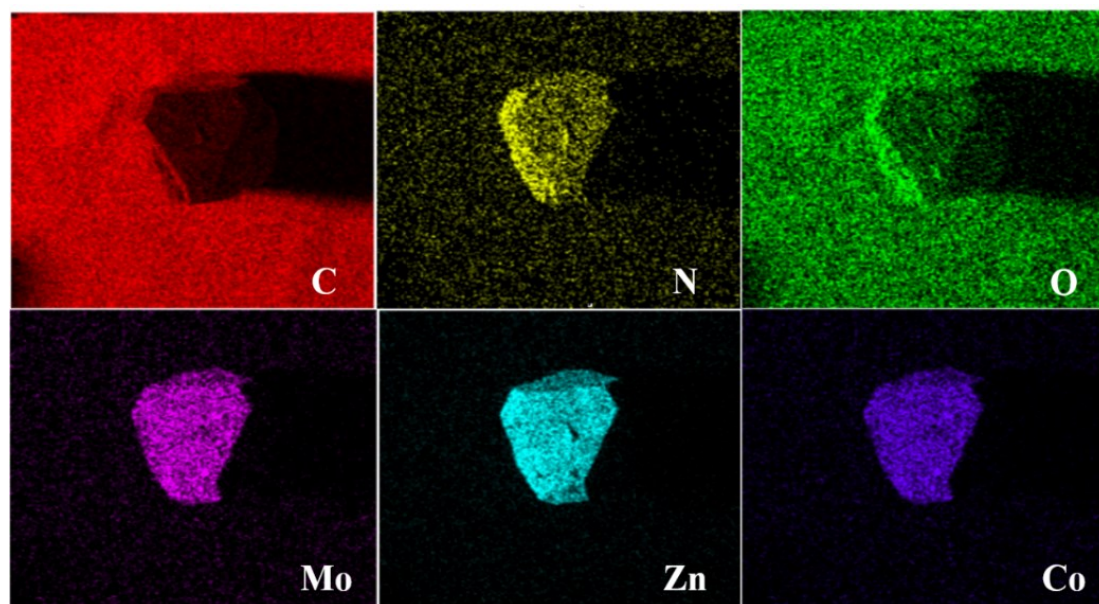


Figure S25. The EDS mapping of Zn/Co/Mo-MOF.

ICP

Table S1. The ICP result of the Zn/Co/Mo-MOF.

Sample	Zn (mmol / L)	Co (mmol / L)	Zn:Co (mol %)
Zn/Co/Mo-MOF	2.3352×10^{-2}	2.3143×10^{-2}	1:1

BET

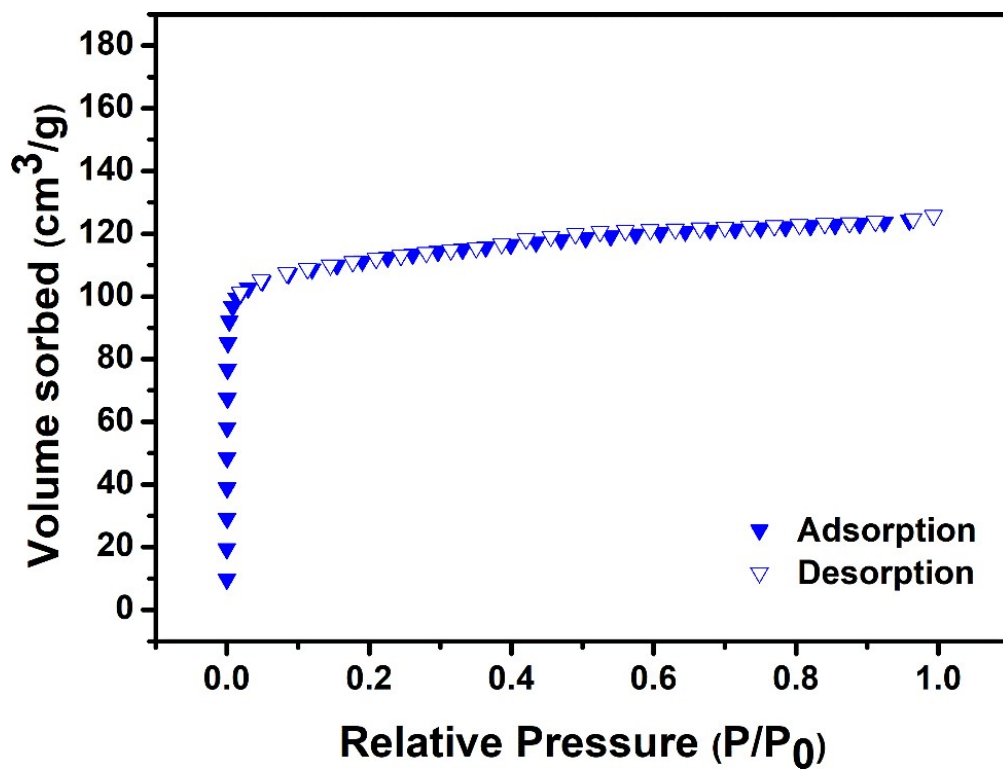


Figure S26. Nitrogen gas adsorption and desorption isotherms for Zn/Mo-MOF.

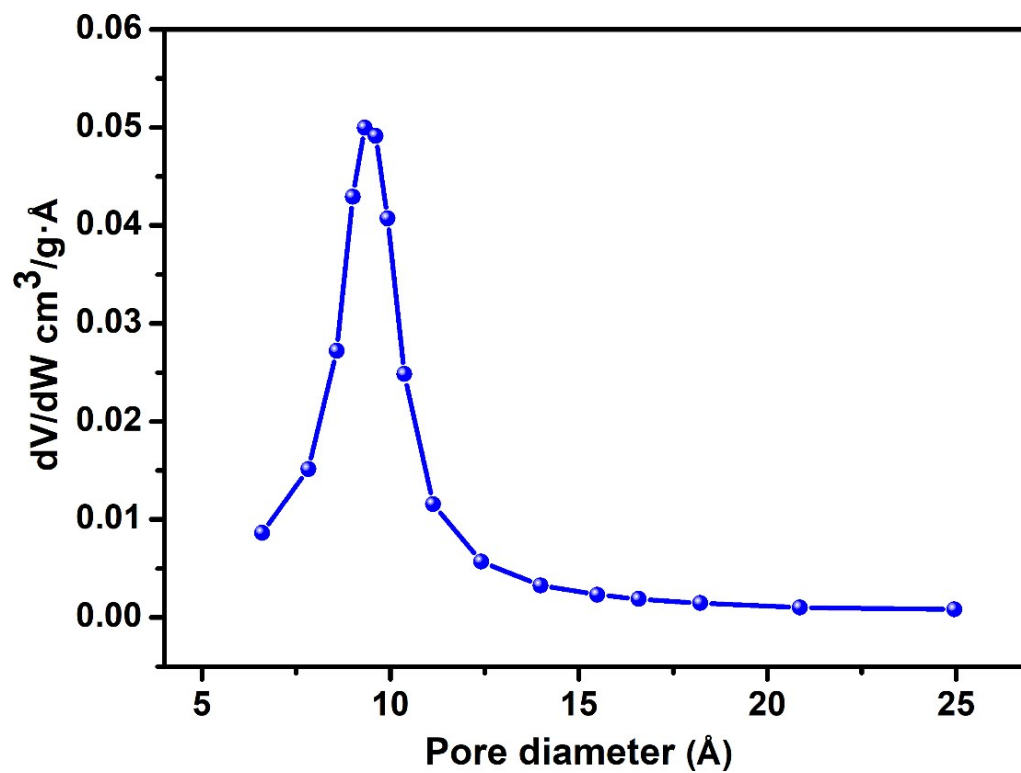


Figure S27. Pore size distribution profiles for Zn/Mo-MOF.

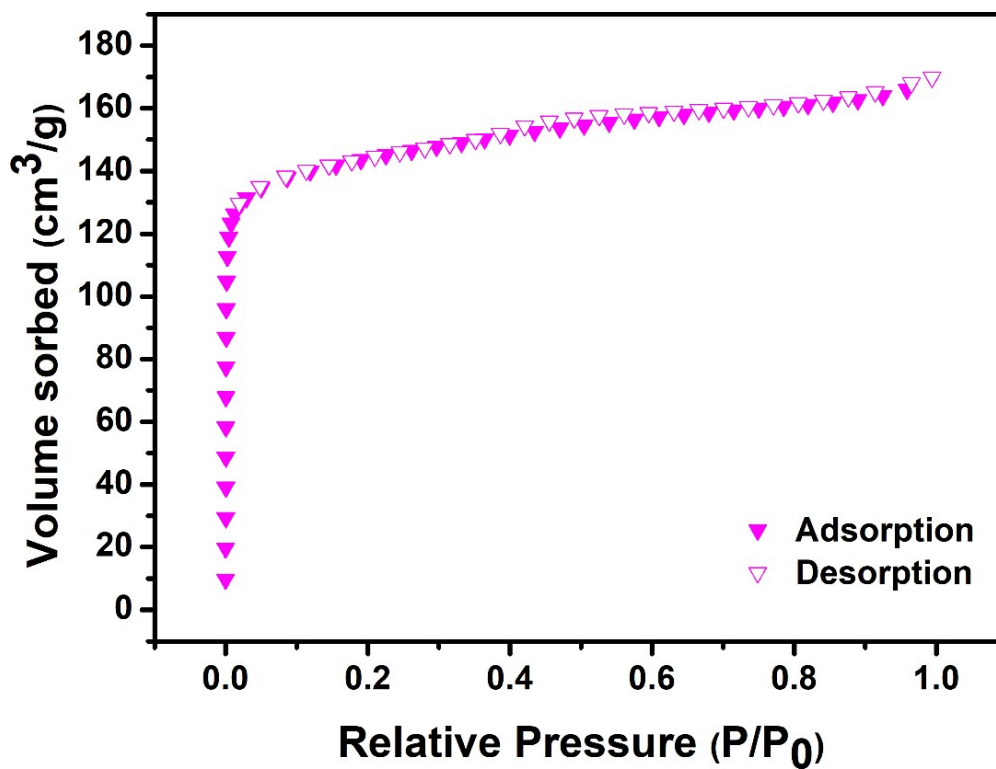


Figure S28. Nitrogen gas adsorption and desorption isotherms for Zn/Co/Mo-MOF.

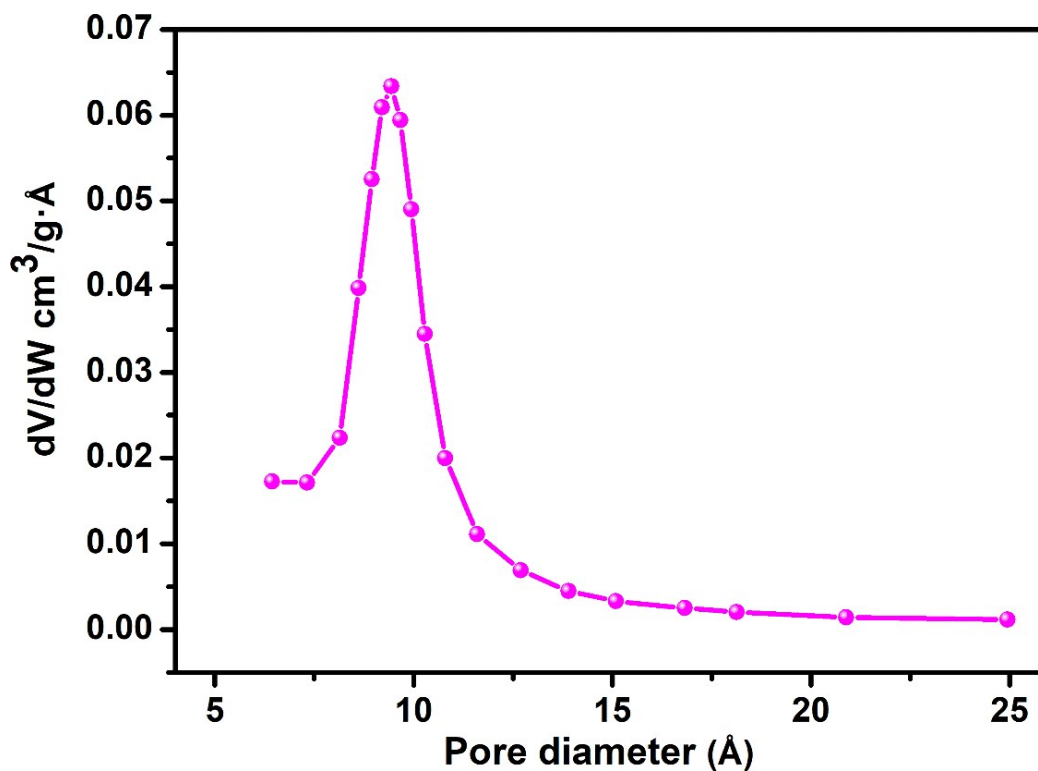


Figure S29. Pore size distribution profiles for Zn/Co/Mo-MOF.

CO₂ Adsorption

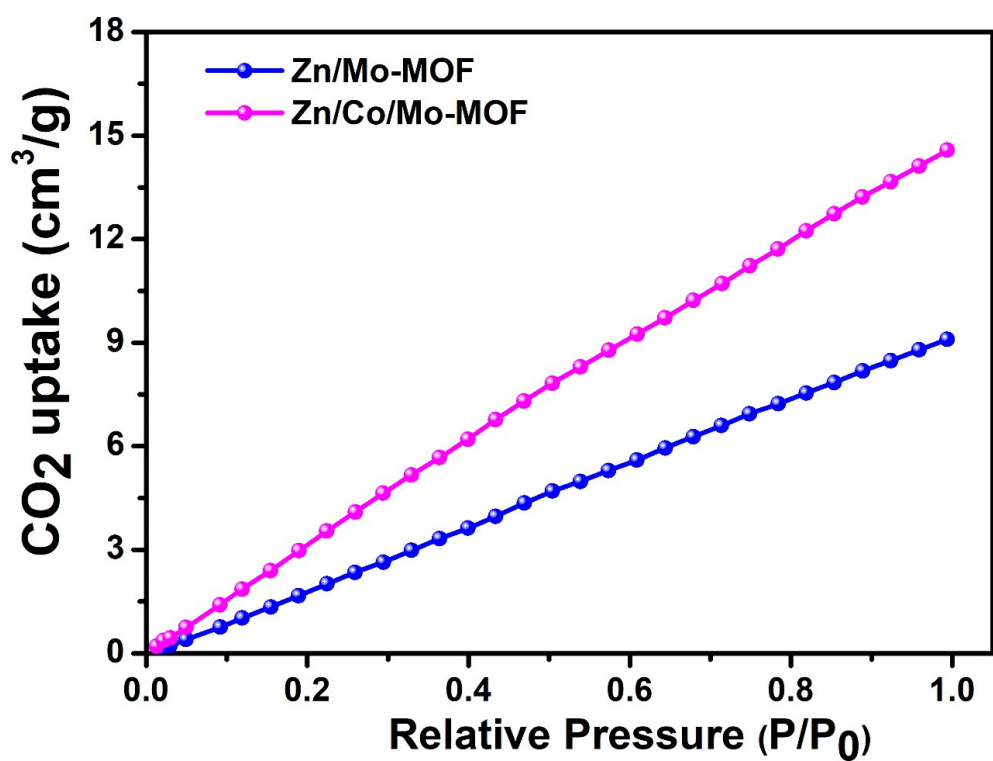


Figure S30. CO₂ adsorption isotherms (298 K, 0 to 1 atm) of Zn/Mo-MOF and Zn/Co/Mo-MOF materials.

Section 3. The Procedure of the CO₂ Photoreduction

Photocatalytic CO₂ reduction experiments.

The photocatalytic performance of **Zn/Mo-MOF** and **Zn/Co/Mo-MOF** was evaluated by applying it to the photocatalytic reduction of CO₂ (CEL-PAEM-D8, AULTT, China). The experiments were carried out in a 100 mL Pyrex flask. A 300 W xenon arc lamp (CEL-PF300-T8, AULTT, China) (photocurrent: 15A) was employed as a visible-light source through a UV-cutoff filter with a wavelength greater than 420 nm, which was installed 10 cm away from the reaction solution. In the system of CO₂ photocatalytic reduction, we put photocatalyst into a mixed solvent of triethanolamine (TEOA, as a sacrificial base) and acetonitrile (1:4 v/v, 50 mL), and used [Ru(bpy)₃]Cl₂•6H₂O (11.3 mg) as photosensitizer. The products were analyzed by performing gas chromatography (GC7920-TF2Z, AULTT, China). The amount of CO and CH₄ was detected by FID, and the H₂ was analyzed by TCD.

$$\text{CO selectivity} = \frac{n(\text{CO})}{n(\text{CO}) + n(\text{H}_2) + n(\text{CH}_4)} \times 100\%$$
$$\text{TON}_{\text{CO}} = \frac{n(\text{CO})}{n(\text{catalyst})} \times 100\%$$

Electrochemical measurements.

The Mott–Schottky spots were carried out at ambient environment via using the electrochemical workstation (CHI 760e) in a standard three-electrode system: The carbon cloth (CC, 1 cm×1 cm) modified with catalyst samples, carbon rod and Ag/AgCl were used as the working electrode, counter electrode and the reference electrode, respectively. The catalyst of 5 mg was grinded to powder and then dispersed in 1 mL of 0.5% Nafion solvent by ultrasonication to form a homogeneous ink. Subsequently, 200 μL of the ink were deposited onto the carbon cloth, and dried in room temperature for Mott-Schottky spots measurements. The Mott-Schottky plots were measured over an alternating current (AC) frequency of 1000 Hz, 1500 Hz and 2000 Hz, and three electrodes were immersed in the 0.2 M Na₂SO₄ aqueous solution.

Photocurrent responsive measurements.

The photoelectrochemical characterizations were performed on the electrochemical workstation (CHI 760e) with the assembled photoelectrodes as the working electrode, the Pt mesh as the counter electrode and the Ag/AgCl as the reference electrode. Meanwhile, the 0.2 M Na₂SO₄ aqueous solution was filled in the cell as the electrolyte. The light source and density were identical with that in the CO₂ photoreduction experiments.

Quantum yield measurement.

The apparent quantum yield (AQY) for products was measured using the same photochemical experimental setup at different wavelengths of 550, 600 and 650 nm. The incident light density was measured using an ultraviolet radiation meter (FZ-A). The calculation of the apparent quantum yield was according to the following equations:

$$\text{AQY} = \text{Ne}/\text{Np} \times 100 \%$$

Ne= 2×number of evolved (CO + H₂ + CH₄) molecules;

Np= the number of incident photons.

Photographs of the CO₂ reduction devices

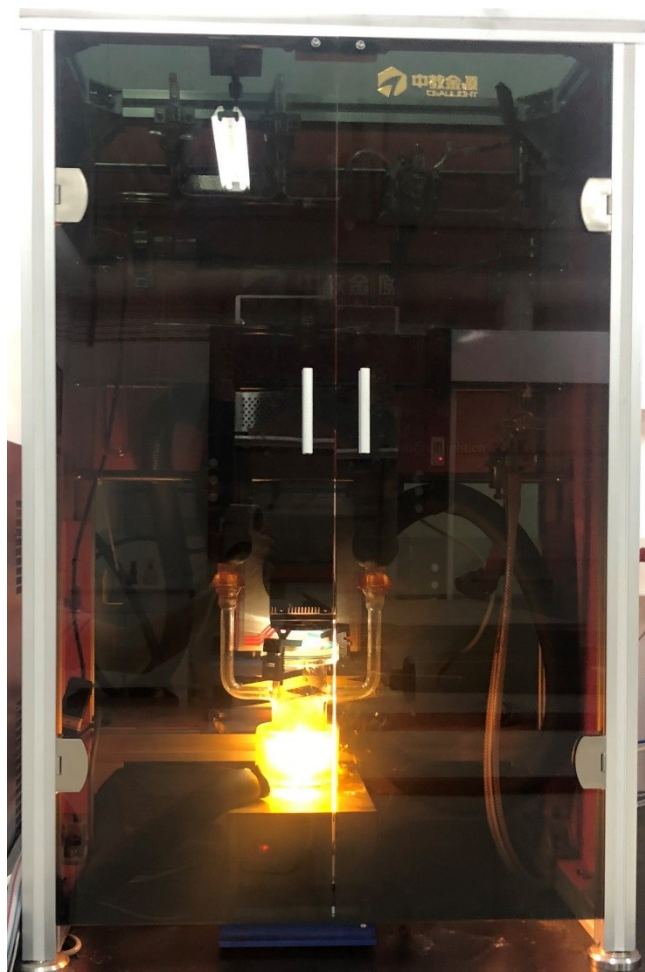


Figure S31. The photograph of the CO₂ photoreduction devices.

Table S2. The AQYs at different excitation wavelengths for Zn/Co/Mo-MOF.

Wavelengths (nm)	Incident light density (mWcm ⁻²)	AQE (%)
550	17.31	0.72
600	17.43	0.77
650	17.28	0.63

Table S3. Research of Reaction Conditions for Zn/Co/Mo-MOF.

Entry	CO (μmol)	H ₂ (μmol)	CH ₄ (μmol)	Rate of CO
-------	-----------	-----------------------	------------------------	------------

1 ^a	230.46	20.3	1.27	38.41
2 ^b	none	none	none	none
3 ^c	1.72	none	none	0.29
4 ^d	1.51	0.22	none	-
5 ^e	none	none	none	none
6 ^f	17.52	3.45	0.82	2.92
7 ^g	none	none	none	none
8 ^h	none	none	none	none

a Reaction conditions: **Zn/Co/Mo-MOF** (5 mg), [Ru(bpy)₃]Cl₂·6H₂O (11.3 mg), solvent (50 mL, MeCN/TEOA, 4/1), CO₂ (1 atm), $\lambda \geq 420$ nm, 25 °C, 6 h reaction time; Rate = n(CO)/time(h); CO selectivity = n(CO)/n(CO+H₂+CH₄) × 100%, where n(CO) and n(photocatalyst) were the amounts of CO (mol) and the catalyst (mol), respectively. b Dark condition. c No [Ru(bpy)₃]Cl₂·6H₂O. d No catalyst. e [Ir(dtbbpy)(ppy)₂]PF₆ replaced [Ru(bpy)₃]Cl₂·6H₂O. f Triethylamine (TEA) replaced TEOA. g H₂O replaced MeCN. h Ar replaced CO₂.

Reaction

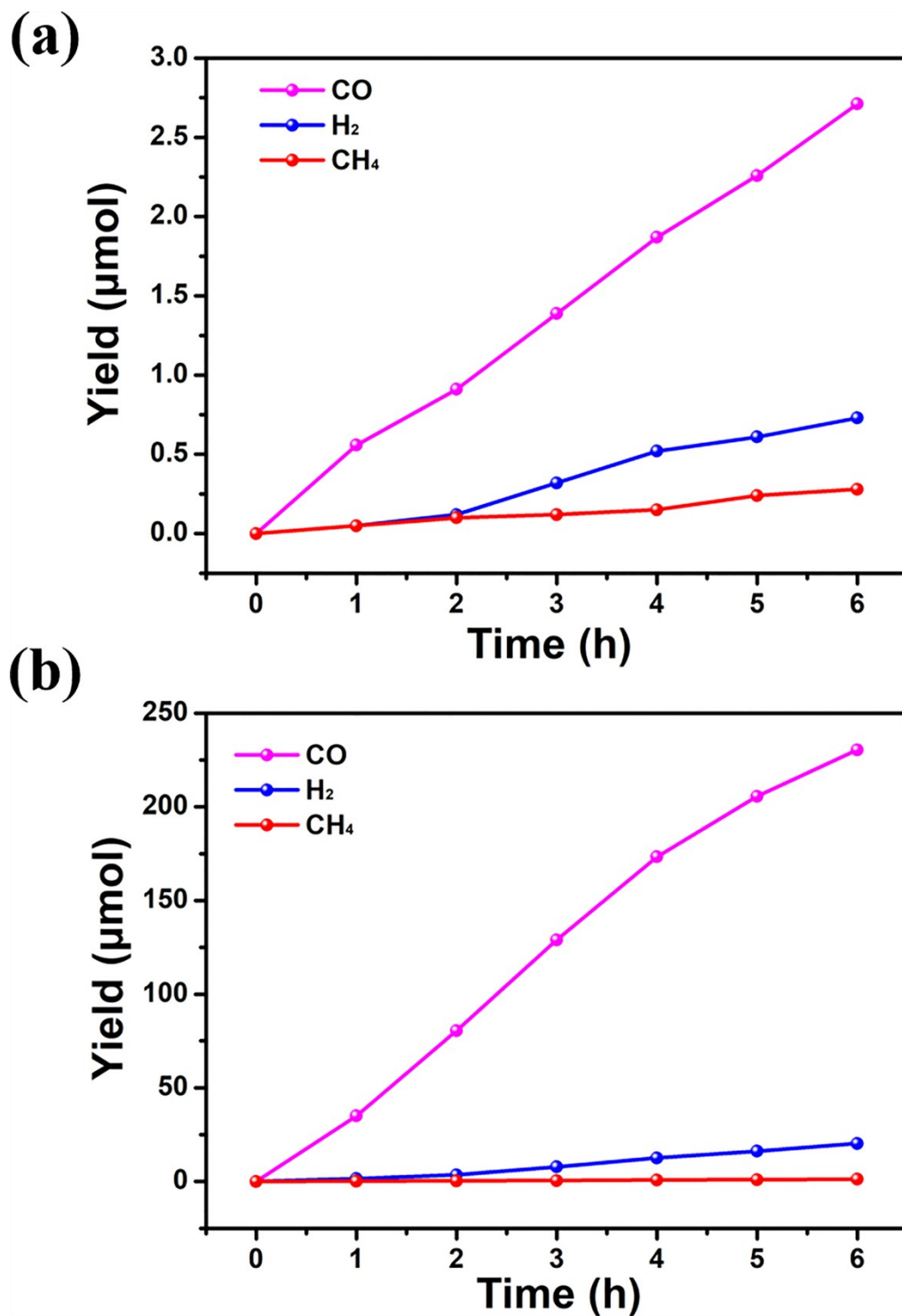


Figure S32. Time-dependent products generation process of (a) Zn/Mo-MOF and (b) Zn/Co/Mo-MOF.

GC profile

The product detected by FID.

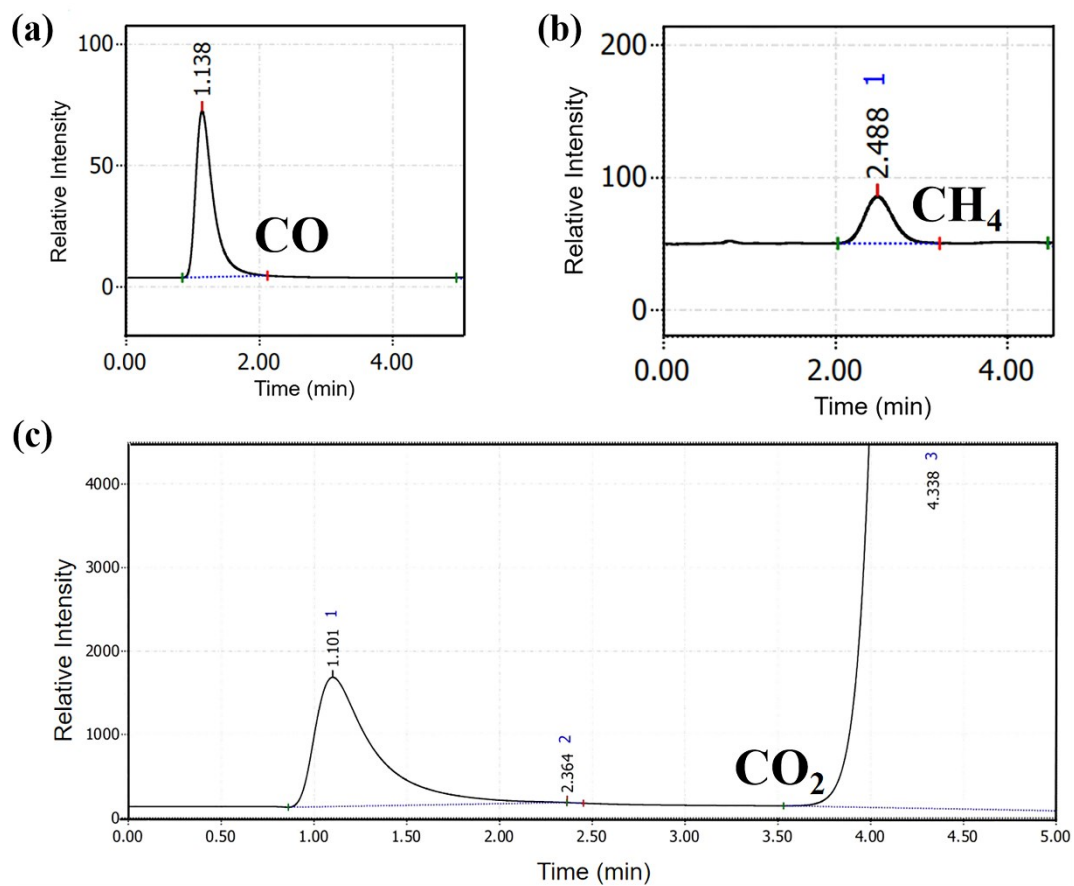


Figure S33. (a) GC profiles of standard CO gas; (b) GC profiles of standard CH₄ gas; (c) GC profiles of CO₂ reduction to CO with **Zn/Co/Mo-MOF** as catalyst after reaction 6h.

The product detected by TCD.

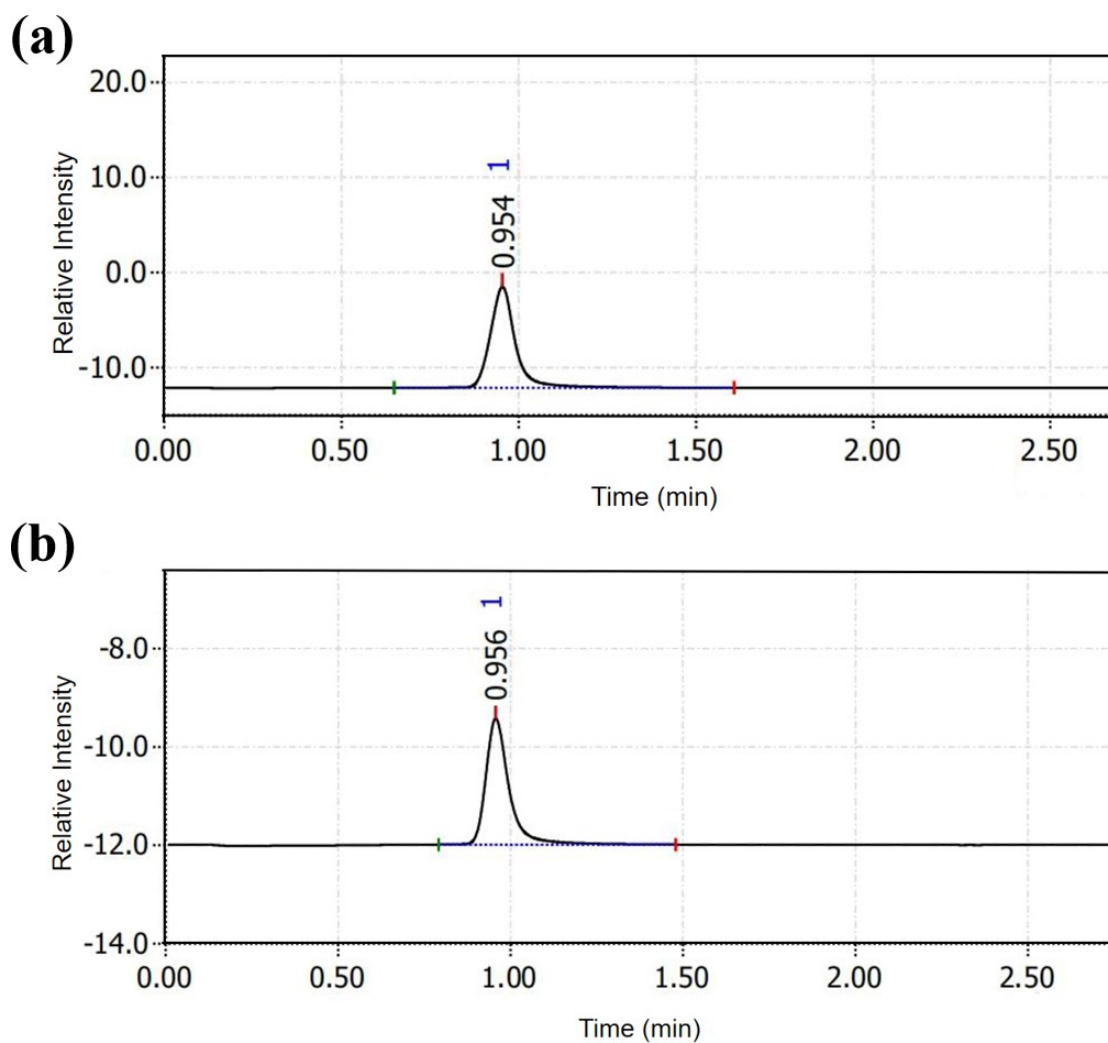


Figure S34. (a) GC profiles of standard H₂ gas; (b) GC profiles of CO₂ reduction to CO with **Zn/Co/Mo-MOF** as catalyst after reaction 6h.

XRD

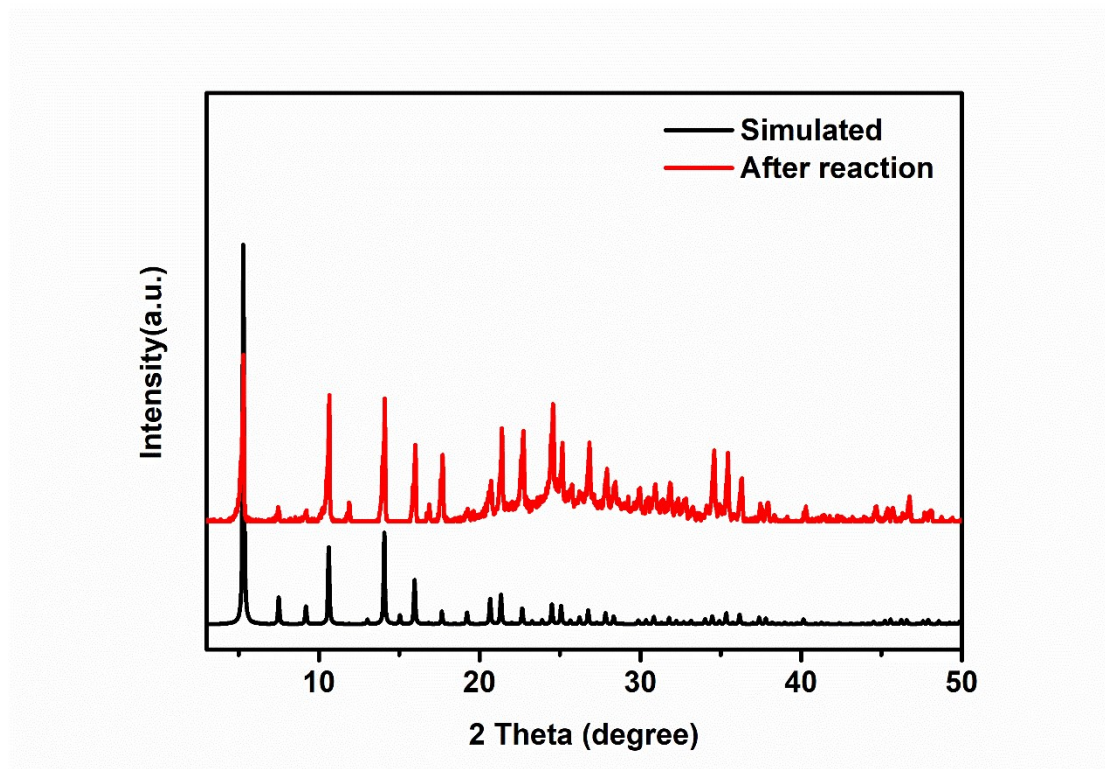


Figure S35. The XRD patterns of **Zn/Co/Mo-MOF** after 4 cycles.

Section 4. Other Tables

Table S4. Selected bond lengths (Å) and angles (°) for Zn/Mo-MOF.

Mo(1)-O(1)	1.719(7)	O(1)-Mo(1)-O(1)#1	107.7(7)
Mo(1)-O(1)#1	1.719(7)	O(1)#3-Mo(1)-O(1)#1	110.4(4)
Mo(1)-O(1)#2	1.719(7)	O(1)-Mo(1)-O(1)#2	110.4(4)
Mo(1)-O(1)#3	1.719(7)	O(1)-Zn(1)-O(2)#4	106.1(3)
Zn(1)-O(1)	1.963(7)	O(1)-Zn(1)-O(2)	106.1(3)
Zn(1)-O(2)#4	1.975(6)	O(1)-Zn(1)-N(1)	106.1(3)
Zn(1)-O(2)	1.975(6)	O(1)-Zn(1)-O(3)	103.0(4)
Zn(1)-N(1)	1.975(6)	O(1)-Zn(1)-N(2)	103.0(4)
Zn(1)-O(3)	2.008(8)	O(2)#4-Zn(1)-O(2)	115.2(5)
Zn(1)-N(2)	2.008(8)	O(2)#4-Zn(1)-O(3)	112.6(2)
O(1)-Mo(1)-O(1)#3	110.4(4)	O(2)-Zn(1)-O(3)	112.6(2)
O(1)#1-Mo(1)-O(1)#2	110.4(4)	N(1)-Zn(1)-N(2)	112.6(2)
O(1)#3-Mo(1)-O(1)#2	107.7(7)		

Table S5. Selected bond lengths (Å) and angles (°) for Zn/Co/Mo-MOF.

Mo(1)-O(1)#1	1.732(8)	O(1)#3-Mo(1)-O(1)	110.5(4)
Mo(1)-O(1)#2	1.732(8)	O(1)#1-Mo(1)-O(1)#2	110.5(4)
Mo(1)-O(1)	1.732(8)	O(1)#3-Mo(1)-O(1)#2	110.5(4)
Mo(1)-O(1)#3	1.732(8)	O(1)#1-Mo(1)-O(1)	110.5(4)
Zn(1)-O(1)	1.957(8)	O(1)-Zn(1)-O(2)	105.6(3)
Zn(1)-O(2)	1.988(6)	O(1)-Zn(1)-O(2)#4	105.6(3)
Zn(1)-O(2)#4	1.988(6)	O(1)-Zn(1)-O(3)	103.4(4)
Zn(1)-O(3)	2.006(8)	O(2)-Zn(1)-O(2)#4	116.3(5)
Co(1)-O(1)	1.957(8)	O(2)-Zn(1)-O(3)	112.3(2)
Co(1)-N(1)	1.988(6)	O(2)#4-Zn(1)-O(3)	112.3(2)
Co(1)-N(2)	2.006(8)	O(1)-Co(1)-N(1)	105.6(3)
O(1)#1-Mo(1)-O(1)#3	107.5(7)	O(1)-Co(1)-N(2)	103.4(4)
O(1)#2-Mo(1)-O(1)	107.5(7)	N(1)-Co(1)-N(2)	112.3(2)

Table S6. The comparison of production of CO for the reported MOF-based materials in CO₂ photoreduction system.

Catalyst	Main product	Side product	Efficiency of main product ($\mu\text{mol h}^{-1}$)	TON _{CO}	Ref
Ni ₃ (HITP) ₂	CO	H ₂	69	82.8	1
Zn/Co/Mo-MOF	CO	H ₂	38.4	39.64	This work
2D-M ₂ TCPE	CO	H ₂	20.9	28.8	2
ZIF-67-3	CO	H ₂	3.9	3.5	3
ZIF-67-1	CO	H ₂	3.8	3.4	
ZIF-67-2	CO	H ₂	3.1	2.8	
Co-UiO-67	CO	H ₂	3.3	49	4
Re-UiO-67	CO	H ₂	0.4	-	
{Co ₃ (TCA) ₂ (dpe) ₃ (H ₂ O) ₆ } _n	CO	H ₂	6.3	15.23	5
{Ni ₃ (TCA) ₂ (dpe) ₃ (H ₂ O) ₆ } _n	CO	H ₂	1.8	7.24	
{Cu ₃ (TCA) ₂ (dpe) ₃ (H ₂ O) ₃ } _n	H ₂	CO	1.1	2.32	
1-DMF	CO	none	0.52	-	6

Table S7. The comparison of selectivity of CO for the reported MOF-based materials in CO₂ photoreduction system.

Catalyst	The amount of CO (μmol)	The selectivity of CO	TON _{CO}	Ref
ZrPP-1-Co	4.14	96.5	-	7
Zn/Co/Mo-MOF	230.46	91.4	39.64	This work
CoOx/MIL-101(Cr)	28.7	70.3	-	8
MOF-525-Co	2.42	85.2	-	9
ZIF-67	37.4	74.2	112	10
Zn-ZIF-8	1.8	47.4	0.4	
Cu-MOF	1.2	44.4	0.7	
Zr-UIO-66-NH ₂	0.9	42.9	1.8	
Fe-MIL-101-NH ₂	4.7	69.1	3.96	
Co ₆ -MOF	39.36	58.3	7.9	

Table S8. The comparison of production of CO for the reported POM-based materials in CO₂ photoreduction system.

Catalyst	Main product	Side product	Efficiency of main product ($\mu\text{mol h}^{-1}$)	TON _{CO}	Ref
Zn/Co/Mo-MOF	CO	H ₂	38.4	39.64	This work
H _{26.5} K _{2.5} Na(H ₂ O) ₁₆ [Ni ₆ (OH)(BO ₃) ₂ (dien) ₂ (B- α -SiW ₁₀ O ₃₇) ₂] ₂ ·24H ₂ O	CO	H ₂	8.14	81.4	12
[Co(en) ₂] ₆ [V ₁₂ B ₁₈ O ₅₄ (OH) ₆] ₁₇ ·17H ₂ O	CO	H ₂	5.7	47.8	13
(H ₂ bbi) ₂ {[Co ₂ (bbi)][Co _{2.33} (H ₂ O) ₄][H _{9.33} CoP ₈ Mo ₁₂ O ₆₂]}·4H ₂ O	CO	CH ₄	4.08	11.2	14
Na ₆ [Co(H ₂ O) ₂ (H ₂ tib)] ₂ {Co[Mo ₆ O ₁₅ (HPO ₄) ₄] ₂ }·5H ₂ O	CO	CH ₄	0.03	0.018	15

Reference

- (1) W. Zhu, C. Zhang, Q. Li, L. Xiong, R. Chen, X. Wan, Z. Wang, W. Chen, Z. Deng and Y. Peng, *Appl. Catal., B*, 2018, **238**, 339–345.
- (2) H. L. Zheng, S. L. Huang, M. B. Luo, Q. Wei, E. X. Chen, L. He and Q. P. Lin, *Angew. Chem., Int. Ed.*, 2020, **59**, 23588-23592.
- (3) M. Wang, J. X. Liu, C. M. Guo, X. S. Gao, C. H. Gong, Y. Wang, B. Liu, X. X. Li, G. G. Gurzadyan, L. C and Sun, *J. Mater. Chem. A.*, 2018, **6**, 4768-4775.
- (4) X. S. Gao, B. Guo, C. M. Guo, Q. S. Meng, J. Liang and J. X. Liu, *ACS Appl. Mater. Interfaces*, 2020, **12**, 24059-24065.
- (5) X. K. Wang, J. Liu, L. Zhang, L. Z. Dong, S. L. Li, Y. H. Kan, D. S. Li and Y. Q. Lan, *ACS Catal.*, 2019, **9**, 1726-1732.
- (6) Q. Li, Y. P. Luo, Y. Ding, Y. N. Wang, Y. X. Wang, H. B. Du, R. X. Yuan, J. C. Bao, M. Fang and Y. Wu, *Dalton Trans.*, 2019, **48**, 8678-8692.
- (7) E. X. Chen, M. Qiu, Y. F. Zhang, Y. S. Zhu, L. Y. Liu, Y. Y. Sun, X. H. Bu, J. Zhang and Q. P. Lin, *Adv. Mater.*, 2018, **30**, 1704388.
- (8) Y. W. Ma, J. Du, Y. X. Fang and X. C. Wang, *ChemSusChem*, 2020, **13**, 1–7.
- (9) H. B. Zhang, J. Wei, J. C. Dong, G. G. Liu, L. Shi, P. F. An, G. X. Zhao, J. T. Kong, X. J. Wang, X. G. Meng, J. Zhang and J. H. Ye, *Angew. Chem. Int. Ed.*, 2016, **55**, 14310-14314.
- (10) J. N. Qin, S. B. Wang and X. C. Wang, *Appl. Catal. B: Environ.*, 2017, **209**, 476-482.
- (11) J. Zhao, Q. Wang, C. Sun, T. Zheng, L. Yan, M. Li, K. Shao, X. Wang and Z. Su, *J. Mater. Chem. A*, 2017, **5**, 12498-12505.
- (12) Y. Chen, Z. W. Guo, Y. P. Chen, Z. Y. Zhuang, G. Q. Wang, X. X. Li, S. T. Zheng and G. Y. Yang, *Inorg. Chem. Front*, 2021, **8**, 1303-1311.
- (13) X. Yu, C. C. Zhao, J. X. Gu, C. Y. Sun, H. Y. Zheng, L. K. Yan, M. Sun, X. L. Wang and Z. M. Su, *Inorg. Chem*, 2021, **60**, 7364-7371.
- (14) J. N. Li, Z. Y. Du, N. F. Li, Y. M. Han, T. T. Zang, M. X. Yang, X. M. Liu, J. L. Wang, H. Mei and Y. Xu, *Dalton. Trans.*, 10.1039/D1DT00809A.
- (15) J. Du, Y. Y. Ma, X. Xin, H. Na, Y. N. Zhao, H. Q. Tan, Z. G. Han, Y. G. Li and Z. H. Kang, *Chem. Eng. J.*, 2020, **398**, 125518.